3
Ground Drilling and Excavation

Alfred William (Bill) Eustes III, William W. Fleckenstein, Leslie Gertsch, Ning Lu, Michael S. Stoner, and Alfred Tischler

3.1
Background

The basis of wealth for humanity is based on natural resources. These include agriculture such as farming, timber, and fishing and minerals such as water, metals, and energy. Since minerals are found primarily in the subsurface of a planet, drilling techniques have been developed to access the subsurface. These include ancient percussion systems to today's modern high-tech rotary drills.

3.1.1
Three Requirements for Any Drilling System

Regardless of the drilling technique, percussion or rotary, three tasks must be accomplished for every drilling system. Those are to:

- penetrate the material
- remove the material
- maintain borehole stability.

Every drilling system must meet those minimum tasks to be successful.

3.1.1.1 Penetrate the Material

Every drilling system must be able to break rock or remove unconsolidated soils from in front of the drill. There are many ways to penetrate rocks and soils. The primary method consists of mechanical breakage of the rock or mechanical movement of unconsolidated soils. The tool used to accomplish the mechanical penetration task is called a bit or head, depending on the industry. Other methods consist of thermal spallation, chemical attack, and melting and/or vaporization.

Drilling in Extreme Environments. Edited by Yoseph Bar-Cohen and Kris Zacny

ISBN: 978-3-527-40852-8

3.1.1.2 **Remove the Material**

Once the rock or soil has been broken, it must be removed. Thus, the rock fragments, called cuttings, or unconsolidated soil must be pushed from in front of the bit to the side. There are two ways to accomplish this, through fluid transport or mechanical transport. Fluid transport means that either a liquid, a gas, or a combination of both flushes the bottom of the borehole. Mechanical transport means that a sweep or blade pushes the cuttings to the side, not unlike a snowplow. Either way, it is imperative to obtain a clean bottom hole for the bit to drill upon or the cuttings/soil will simply be reground into finer particles, using valuable drilling energy in the process, and slowing the drilling penetration.

The cuttings/soil must be removed from the side of the bit to either the surface or to an open area within the borehole. This can be accomplished by the same methods as for removing material from the bottom hole: fluid or mechanical transport. Typically for most commercial drilling operations, a fluid; either pneumatic, liquid, or a mixture of both, is pumped down through a pipe (often called a drill string), through the bit, and up the annulus. This brings the cuttings/soil generated at the bit out of the borehole to the surface. There are a few systems that can compact the cuttings into the borehole wall. This is typically for unconsolidated formations. Often, the energy needed to recompact the cuttings/soil, which will never reach the same density as *in situ*, into the borehole wall can be enormous.

3.1.1.3 **Maintain Borehole Stability**

Once a borehole has been created, it must be maintained until the borehole has no further use. The life of a borehole can be so minimal as simply to allow immediate access to the subsurface or it can even be a century for resource acquisition, depending on the need. This support can be easy for hard, consolidated rocks; they are hard enough for self-support. No further efforts need be made to keep the borehole open. However, this can be difficult with soft, unconsolidated rocks that tend to fall into the borehole. In addition, fluid flow into borehole can instigate borehole collapse. In either case, or in any other situation that threatens the integrity of the borehole, this is called borehole instability. In these situations, there are two methods to keep the borehole open in a controlled environment: either fluid support or mechanical support, or both.

While drilling a well, the primary source of borehole support for borehole instability is resistive pressure inside the borehole. The easiest way to accomplish this, at least on Earth, is through hydrostatic pressure from a fluid column. This fluid column is called a drilling fluid and is often called "mud" in industry as the primary constituents of this fluid are clay and water. Actually, any pressure in a borehole can be used to support the borehole; however, fluids in a gravity field will act more like the fluid pressures and tectonic stresses in the borehole wall. This makes fluid pressure at least balance the pressures as the well depth increases. However, if the pressure inside the borehole is too high, the rocks can fracture, leading to the loss of fluid into the formation and the subsequent lowering of the hydrostatic head. This can cause the borehole support pressure to decrease below the minimum values, leading to borehole collapse. This is also the result of too low a pressure inside the borehole.

A more permanent method of borehole support is mechanical. A pipe, often called casing, is lowered into the hole. The material of the casing is usually steel, but can be plastic or fiberglass if the borehole stresses are not greater than the mechanical strength of the material. The annular area between the borehole wall and the pipe can be filled with a cementaceous material. This limits fluids migration behind the casing and supports the casing by distributing the formation pressures and tectonic stresses into the casing. For weaker formations, sometimes a mesh can be used. Regardless of the method, this casing will permanently maintain borehole stability until abandonment, assuming that the casing was designed properly. This design process can be significant, however. Successful installation of casing contributes greatly to methods of completing a well for producing a resource or accepting fluids for injection into the subsurface for disposal or recharge. The casing can keep access to a borehole open.

3.1.2 Types of Earth Boreholes

On Earth, there are many reasons to bore into the planet. The oldest reason for drilling was for fresh water and, in some cases, salt water (for the salt). The ancient Chinese and Mesopotamians drilled wells 3000 years ago. Mankind has been continually drilling for water. In fact, the leading cause of longevity in the twentieth century was fresh and clean drinking water, usually from boreholes drilled in the Earth (Dunnigan, 1999).

However, most boreholes drilled in the Earth today are for the production of hydrocarbons. Literally hundreds of thousands of wells are drilled around the world each year. These wells can run from 100 to 6000 m in vertical depth for hydrocarbon production (although some boreholes have been drilled to 10 000 m looking for hydrocarbons) and can be as long as 10 000 m in directional holes. They are found from the Arctic to the equator and from high terrains to 3000 m water depths. Typically, hydrocarbons are found in sedimentary rocks and, therefore, the drilling technology is designed for sandstone, limestone, shale, and other sedimentary types of rocks. These rigs are designed for time efficiency and low-cost operations. They also have equipment available to mitigate environmental damage and for well control events.

Many holes are drilled in mining. These can be surface holes for analysis and blasting to *in situ* holes within underground mines for assaying, structural support, and blasting. Often, mining takes place not only in sedimentary rocks, but also in harder igneous and metamorphic rocks. Mining drilling, while similar to hydrocarbon drilling in some respects, has different types of drilling equipment and drilling bits designed for confined spaces underground and harder formations.

Other boreholes are used to access geothermal resources. In this drilling process, not only are the rocks typically harder than in hydrocarbon drilling, but also much hotter, on the order of 350 °C. These operations are similar to hydrocarbon drilling operations, only hotter!

Other holes are drilled for underground environmental damage assessment and environmental disposal of hazardous waste products. For example, chemical waste is often injected into deep strata for disposal. In addition, there is discussion regarding carbon sequestration to mitigate carbon dioxide climate change. Many holes were drilled at Yucca Mountain in Nevada to study the mountain for suitability for nuclear hazardous waste disposal.

Finally, another reason to drill is to acquire scientific knowledge. Such drilling may be in rocks, for example the International Continental Scientific Drilling Project (ICDP) on land, and Joint Oceanographic Institutions for Deep Earth Sampling (JOIDES) offshore. Others are drilled into earthquake fault zones to understand better the nature of fault movement and earthquakes, such as the SAFOD project. They are also drilled in ice sheets from the highest glaciers to the Antarctic ice sheet such as the West Antarctic Ice Sheet Divide Ice Core (WAISCORE). The deepest holes in Earth are for scientific purposes. The Russians drilled a hole 12 000 m deep in the Kola Peninsula in the late 1980s and early 1990s.

3.2 Drilling Rigs

Drilling rigs are primarily of two types: percussion and rotary. Percussion drilling is the application of repeated impacts upon the rocks to effect penetration. This is the ancient technology of the Chinese and Middle-East civilizations (Brantly, 1971). Newer styles of percussion rigs include rotary percussion and sonic rigs. Rotary drilling is the process of rotating a bit either to crush or to scrape the rock for penetration. Of these, rotary is the dominant style of drilling rig in water, geothermal, and especially hydrocarbon operations. Percussion rigs are often used in civil engineering applications.

3.2.1 Percussion Drilling Rigs

3.2.1.1 Cable Tool Drilling Rigs

Cable tool rigs are drilling machines that use impact mechanisms for their primary drilling operation. The oldest drilling rigs are of this style. These ancient rigs typically consisted of a weight tied off on to a tree. The tree was laid horizontally to the borehole and tied down on one end. There was a pivot point set up nearer to the tree tie down position than to the other end. This allowed the other end the tree to flex. The weight was tied off to the other end of the tree. Then someone literally jumped up and down (or at least pushed and pulled) on the flexible end, which reciprocated the weight up and down. With the length of the rope tying the weight back to the tree set to the correct length, the weight would strike the rocks, breaking them into pieces, called cuttings, and extending the hole deeper. These types of rigs predominated in late nineteenth and early twentieth century drilling operations in oilfields. A more sophisticated machine than a tree was the cable-tool rig. Since California was initially explored for hydrocarbons at about the same time as the advent of the cinema, often Hollywood's version of the oilfield is based on this style of rig (Figure 3.1).

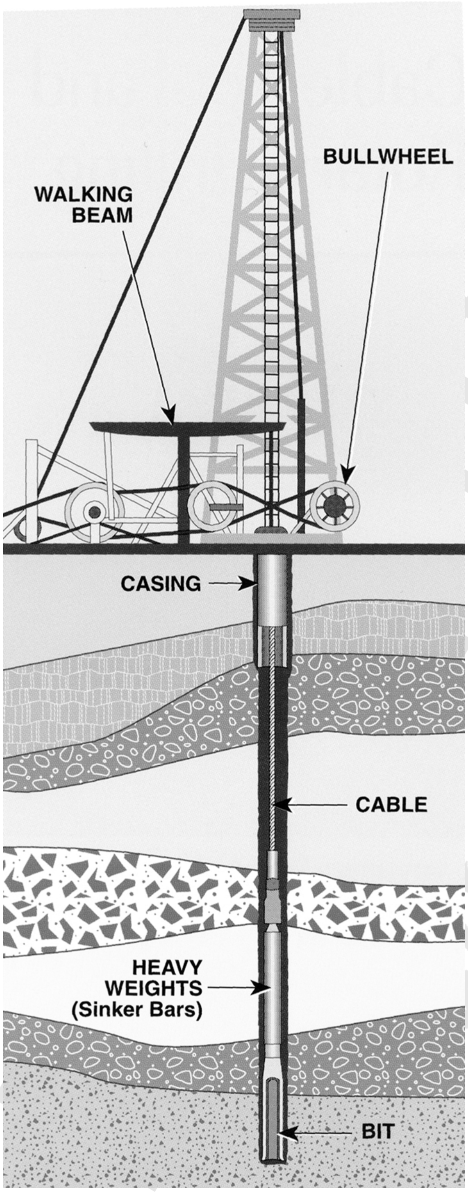

Figure 3.1 Cable tool rig. Courtesy PETEX.

With this rig, a heavy weight is reciprocated up and down in the borehole, typically not more than a few meters. This bit impacts the bottom of the hole, breaking the rock into cuttings of various sizes. The bits are heavy weights with a chisel type of tooth on the bottom. The bit is suspended by a wireline, hence the name "cable-tool." The bit diameter ranges from 24 to less than 6 in.

Eventually, the cuttings must be removed or the bit will continue to pound the previously pulverized rocks. The bit wireline is reeled back on to its spool at the surface and a bailer is lowered into the hole on its own wireline. The bailer taps the bottom of the hole, opening a lower pressure chamber, allowing the cuttings to be pushed into the chamber. The bailer is brought back to the surface, where it is dumped off to the side of the rig and examined. If not all of the cuttings were returned (since the volume is known from the penetration), the bailer is run back into the hole until the bottom is reasonably clean. Then the bit is lowered back down the hole and the drilling process is started again.

This style of rig has advantages and disadvantages. The advantages include lower power requirements and underbalanced drilling. Most of the old cable-tool rigs had low power steam engines of 15–30 kW. Not much power is required to lift and lower the bit and bailer. Also, since not much power was needed for anything else, these rigs could be small. In addition, the hole is not full of liquid. This means that the pressure in the borehole is typically less than the pressure in the formation, which is called an underbalanced situation. If the pressure in the borehole from the hydrostatic head of a full column of fluid is higher than the formation pressure, this is called overbalanced. If the hole was full, the bit would tend to float, not allowing penetration. In addition, the lower borehole pressure assists the cuttings to break as they are not being held down by hydrostatic pressure in the borehole. A hole that is not full has the advantage of not causing formation damage such as fines migration, clay swelling, and chemical reactions. However, typically, a 2–3 m cushion of water was used on the bottom to allow the cuttings to disperse, making them easier to collect.

This same advantage of low fluid levels is a disadvantage in the case of high formation pressures. If there is a pore space fluid in the rock that is mobile, there is permeability for that fluid to flow through the rocks, and if the pressure in the borehole is lower than that in the formation, the fluid will flow uncontrolled into the borehole. This is called a “kick.” If the kick is not brought back under control, the well will have an uncontrolled flow out of the borehole, called a “blowout.” This is a very photogenic event and hence why Hollywood’s movie rigs are shown blowing out (even though it is a relatively rare event today). With cable-tool rigs, however, this underbalanced situation is naturally part of the process, hence these operations often did produce blowout.

Another disadvantage is the batch process nature of drilling. The bit is lowered into the hole, the hole is drilled some distance, and the bit is retrieved. Then the bailer is lowered into the hole, collects the cuttings, and is brought back to the surface and dumped. This is a non-continuous process that is not particularly efficient if one is drilling a hole. There are times where this is not an issue, such as in continuous coring operations.

Another disadvantage with the lack of fluids in the borehole concerns borehole support. Without fluid, the borehole will not be supported by fluid pressure. This is not a major issue in hard, consolidated rocks. However, in softer rocks, it is a serious problem. The famed Spindletop well near Beaumont, TX, drilled at the turn of the twentieth century, was undrillable with cable-tool rigs, as the rocks were too unconsolidated, and the borehole continued to collapse. However, with the application of rotary rigs, this was overcome and the well was successfully drilled.

3.2.1.2 Rotary Percussion Hammer Rigs

Rotary percussion hammer drills employ a reciprocating piston to produce impact energy that is transmitted through a bit to break rock. They are particularly well suited to drilling medium-hard and hard rock and are arguably the most rapid commercial hard rock drilling method. The two basic types of percussion hammer drills used in industry are the top hammer (TH) and the down the hole hammer (DTHH). Both techniques rotate the drill string to index the bit's rock-breaking elements (inserts) over fresh rock surface between impact blows. Absence of rotation during drilling results in embedding of the bit inserts up to the bit face, at which point penetration ceases. The application of a downward force on the drill string is required to translate the bit into the rock prior to piston impact in order to ensure efficient coupling of impact energy. Poor coupling of the rock and bit during impact results in reflection of impact energy, mostly or entirely back up the drill string.

Top hammers are primarily used in the construction and mining industries to drill blast holes up to 0.23 m in diameter. Top hammers are usually hydraulic fluid-powered devices in which a piston is cyclically accelerated into a component used to connect the hammer drill to the drill string, called a shank adapter. The energy transmitted to the shank adapter is calculated as (Clark, 1979)

$$E_{\mathrm{p}} = \frac{1}{2} m_{\mathrm{p}} v_{\mathrm{p}}^2 T_{\mathrm{r}} \tag{3.1}$$

where m_{p} is the piston mass, v_{p} is the piston velocity, and T_{r} is the energy transfer coefficient.

The stress wave produced by impact of the piston with the shank adapter propagates through the entire drill string, ultimately causing the bit to accelerate into and break the rock. Typical top hammer impact frequencies range from 50 to 100 Hz. Power delivered to the drill string is calculated as

$$P = E_{\mathrm{p}} f \tag{3.2}$$

where P is the hammer power and f is the hammer cycle frequency.

Compressed air or water is circulated through the drill string and bit to remove reduced rock from the cutting surface to minimize rock re-breaking and clean the hole. This technique tends to be limited to depths on the order of 50 m because of energy transmission losses of 2–6% between jointed drill pipe connections.

DTHH drills are located in the borehole at the bottom of the drill string. The bit is directly coupled to the hammer drill assembly and therefore this technique is not limited by the energy transmission losses characteristic of the TH technique. DTHH technology is routinely used in the mining, construction, oil and gas and water well drilling industries to drill holes up to 1.2 m in diameter. As for the TH method, a free-flying piston is used to create impact energy. Reciprocation of the piston is powered by a fluid delivered through the drill string and regulated by porting in the piston and hammer case assembly. In some devices, valving is used to control fluid flow. The piston in the DTHH directly impacts the bit shank.

Most DTHH devices in commercial use are pneumatically powered, although prototype "mud"- and water-powered hammers have recently been developed. The fluid used to power the piston exits through the bit to clean the cutting surface and remove debris from the hole. Typical commercial operation input air pressures to the hammer range from 200 to 500 psi with impact frequencies from 15 to 40 Hz. Borehole depths up to 4500 m have been drilled with DTH hammers using high-compression air boosters. The piston impact energy and drill power can be calculated in the same manner as for TH drills.

3.2.1.2.1 **Rotary Percussion Drill Bits** The two primary bit types used with rotary percussion hammers are chisel or cross bits and button bits. Both bit types possess rock-breaking features designed to produce stress concentrations at the rock–bit interface. Chisel or cross bits are descended from jack-hammer bits and possess wedge-shaped inserts that are usually soldered in cavities in the bit body. They tend to be more difficult to manufacture and install in the bit body, have comparatively low impact energy limitations and tend to have lower penetration rates than button bits. They are limitedly available for top hammers but have largely been abandoned by DTHH manufacturers due to the higher impact energies produced by modern DTH hammers.

Button bits are comprised of numerous hemispherical, parabolic, or conical profile elements, called buttons, which are pressed into machined holes in the bit body. They tend to be spaced along circles at different radii from the bit center in either symmetric or asymmetric arrangements. Sharper profiles, such as conical and parabolic, are used in softer formations to increase the penetration depth per blow, whereas rounder profiles, such as hemispherical, are used in harder formations because they are more rugged and less susceptible to impact damage. Buttons are typically made of tungsten carbide or tungsten carbide coated with polycrystalline diamond (PCD) where increased wear resistance is desired.

3.2.1.2.2 **Rotary Percussion Drilling Rigs** TH rigs are generally specialized units custom designed for the unique mounting location of the top hammer above the drill string. The TH drill rod is also uniquely designed and manufactured to minimize the energy transmission loss between joint connections. The drill rod is fed through a sealed enclosure called a dust collector or diverter with a discharge line to direct rock cuttings and ejected drilling fluid away from the borehole and the rig. A cyclone separator is sometimes used to separate solids from the fluid stream.

DTH hammers are compatible with the conventional rotary rigs and drill pipes used with rolling cutter and drag bit technology.

3.2.1.2.3 **Resonant Sonic Drilling Rigs** Another type of percussion system is the resonant sonic drilling rig, sometimes called the "rotasonic" or just "sonic" drilling method. This type of drilling was investigated by Soviet workers in the 1940s. However, the current rig type was developed in the 1950s and 1960s. This type of rig is used in subsurface environmental sampling and in ground water monitoring, and also in other shallow hole needs.

The resonant sonic drilling rig operates on the principle of sonic energy transmission. The energy is input into a pipe from a set of counter-rotating weights connected to the top of the pipe and staying above ground level. The rotating weights are perpendicular to the pipe axis. As they rotate, they impart a motion along the pipe axis. Perpendicular vibrations are canceled by the counter-rotation of the weights. When the frequency (between 50 and 120 Hz) of the input waves matches the natural frequency of the pipe under given boundary conditions, the energy is efficiently conveyed to the bottom of the pipe. The bottom of the pipe, which can be a bit or even just the end of a pipe, drills through whatever might be in the way, including boulders in soils. It has been shown that these types of drills are very fast compared with conventional rotating drilling systems (Swanson, 1994).

For this type of drilling operation, typically there is no drilling fluid, nor are there any auger flights. In that situation, the cuttings generated at the bottom end of the pipe are not brought to the surface. It is thought that the vibrations from the pipe liquefy the borehole cuttings and wall, allowing for the packing of the cuttings into the wall. For a hollow pipe, this leaves a pristine core, since there is no fluid circulation to wash the core. Nor are any contaminants brought to the surface other than what is on the pipe as it is withdrawn from the hole. However, fluids can be used to help speed up the drilling process. In that case, some of the cuttings are transported to the surface. It is reported that only 20–30% of the cuttings are brought to the surface, as opposed to rotary or cable tools systems. The pipe can be left in the hole as casing if retrieval is not an issue. However, difficulties can arise with these systems. As noted, the boundary conditions of the system are important. Provided that there is an energy sink using most of the energy from the vibration input, the pipe will not self-destruct from resonance. However, if for some reason the vibration input energy is not absorbed somewhere other than the pipe, the pipe will have stresses that build up quickly to beyond the ultimate strength of the material and will fail, potentially catastrophically. In addition, in hard rocks such as granite, the bit can wear out quickly from the frequency of impacts and a drilling fluid is needed to help with the drilling (Boart Longyear).

3.2.2
Rotary Drilling Rigs

The primary type of drilling rig used today is the rotary drilling rig. In this style of rig, drilling is accomplished by applying a force to rotate the bit in the desired direction of penetration. The bit is at the end of a hollow pipe, called the drill string. Drilling fluid can be circulated down the inside the pipe and up the annulus of the borehole and drill string.

Applying a force to the bit perpendicular to the face of the borehole floor initiates the drilling process. As noted in previous and upcoming sections regarding how the drilling process operates, the application of this force penetrates the rock face, breaking it into cuttings. Rotating the bit allows for continuing application of the force over differing sections of the rock face as the bit rotates against the rock face.

The drill string connects the bit back to the surface. At the bottom of this drill string are thick-walled pipes, called drill collars, which resist bending when the force is applied to the bit. Otherwise, the forces would cause too much flexing of the drill string, leading to fatigue failures. As will be noted later, this bottom section of the drill string is called the bottom hole assembly and contains not only the drill collars, but many other useful tools for drilling.

As noted earlier, the drill sting is hollow. This allows for a fluid to be pumped down the inside of the drill string and out of the bit. This fluid carries the cuttings generated by the bit up inside the annulus and out of the hole.

A huge advantage of rotary systems is the ability to control the energy level during drilling. Since the rotational speed and bit force can be varied significantly, the application of energy to the drilling process is infinitely variable. The more energy that is applied to drilling processes (although it can be overdone, damaging the borehole), the faster the rock is penetrated. On Earth, “time is money”, so drillers tend to overwhelm the hole with energy, making the drilling faster. This is the primary reason why rotary drilling is the dominant style of drilling rig.

Another advantage of rotary drilling over percussion drilling is that the drilling process is continuous. Since the drilling fluid is circulated from the surface to the bit, picking up cuttings at the bit and then transporting them out of the hole, there is no need to stop and clean the hole as is done in percussion drilling. It is a continuous process and is significantly more efficient for drilling operations. However, if the cuttings transport capability of the fluid is exceeded by the cuttings generation, then there can be difficulties in keeping the hole clean. The drill string could even become stuck in the borehole.

Because the drilling fluid is circulated, it is inherent that the fluid completely fills the hole. This means that a continuous column of fluid is against the borehole face, supporting the borehole. It also means that the fluid exerts a hydrostatic pressure at all points in the borehole. If this pressure is greater than the fluid pressure in the rocks, overbalanced conditions, then the well will not kick. However, if the borehole pressure does decrease below the formation pressure (and there is fluid and permeability), then a kick will still occur. With rotary drilling, however, since there is a full fluid column, the process to bring the borehole back under control is relatively simple.

A disadvantage is that the equipment for rotary drilling is heavy and complex. There is a drill string that must have enough strength to support itself and also to contain hydraulic pressure. The equipment needed to lower and hoist the drill string and casing is heavy and powerful. The power needed to circulate the fluid, hoist the drill string, and rotate the string is significant. Even the smallest rotary drilling rigs need about 300 kW and many rigs have 4000 kW power, just for the hoisting equipment alone.

There are two primary types of rotary drilling rigs used in hydrocarbon drilling applications: the coiled tubing drilling rig and the standard rotary drilling rig that rotates pipe.

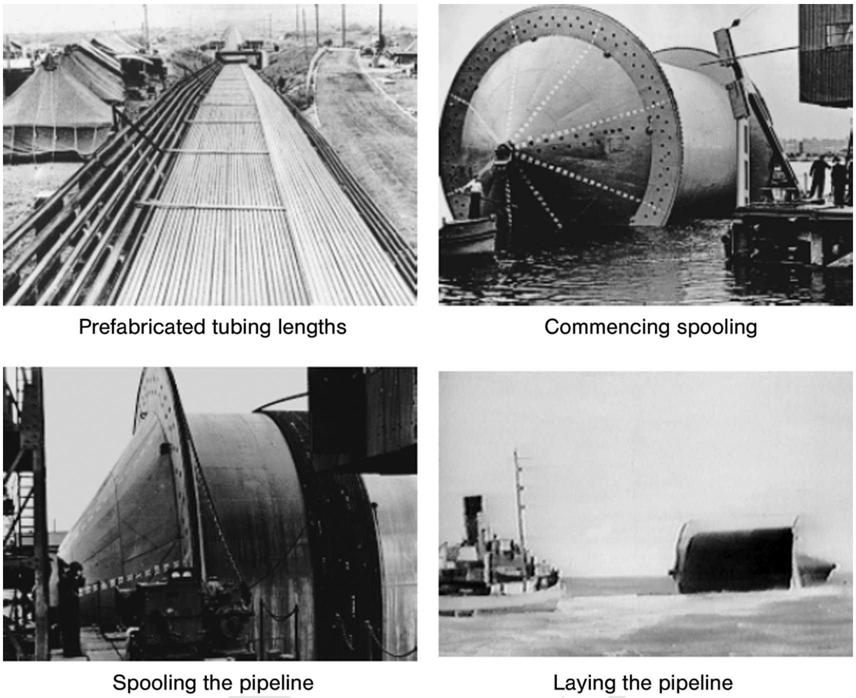

Figure 3.2 Project PLUTO.

3.2.2.1 **Coiled Tubing Drilling**

The origins of coiled tubing began with Project PLUTO (PipeLines Under The Ocean)(see Figure 3.2), in which a total of 23 pipelines were welded together out of 20 ft joints of 3 in which were spooled together on floating drums that were 40 ft in diameter and 70 ft in width. The pipelines, approximately 70 miles long, were then laid across the English Channel in support of the 1944 invasion by towing the drums across the channel while the pipeline unspooled.

The first coiled tubing unit was developed in 1962 by Bowen Tools by fabricating a 15 000 ft, 1 3/8 ft tubing string from butt-welded 50 ft sections, which was spooled on to a 9 ft diameter reel. The injector was based on two contra-rotating chains, similar to today's designs, with a simple stripping rubber to seal around the tubing, and was based on a design developed by Bowen Tools for submarine radio antennas.

Coiled tubing units have undergone continuous improvement, with the fabrication of larger diameter coiled tubing that can be milled continuously to the desired length, minimizing welds. Better metallurgy and better welding technology have eliminated most of the tubing failures that plagued early coiled tubing operations. Most of the steel tubing in commercial applications comes from two manufacturers, Precision (Tenaris) and Quality Tubing (Varco). The tubing is made at several manufacturing stations synchronized to form and weld steel strips into tubing on a continuous basis. It comes in a range of alloys with tensile strength from 70 000 to 120 000 psi and sizes from 1 to 4.5 in o.d.. Several companies make fiberglass coiled tubing, some with fibers for communication, but none are in commercial use at present. Halliburton's Anaconda Project was the most recent attempt, using composite tubing manufactured by Fiberspar, but after several field trials, the system has been mothballed.

A 2005 survey by the International Coiled Tubing Association (ICoTA) indicates there are approximately 1182 coiled tubing units worldwide. Internationally, there are 614 rigs. They are distributed in the Middle East (128), Europe/Africa (143), South America (107), and the Far East (236). North America has the rest.

A typical coiled tubing unit will be trailer mounted with a tubing reel, coiled tubing, hydraulic crane for deployment, a hydraulic injector head, with stripping rubber and quad blowout prevention (BOP) equipment for deployment directly to the wellhead (Figure 3.3).

The heart of the coiled tubing unit is the injector head (Figure 3.4), which is composed of opposing, hydraulically activated chain drives, which grip the tubing, and either inject it into the well under pressure or provide force to prevent the tubing from falling into the wellbore.

The first coiled tubing drilling rigs were developed independently in 1964 by the French Petroleum Institute and the Cullen Research Institute, and in 1976 the Canadian company Flextube developed and commercially operated a coiled tubing drilling system for several years. The modern coiled tubing drilling era began in 1991, as larger coiled tubing, such as 2 and 2 3/8 in, were developed. Coiled tubing drilling has several advantages over conventional drilling operations, such as

- ease of pressure control, facilitating underbalanced operations
- smaller surface footprint with reduced rig up time
- faster tripping speeds.

Coiled tubing drilling can be divided into non-directional and directional wells. Non-directional wells are the majority of wells drilled with coiled tubing and use conventional drilling assemblies based on hydraulic mud motor technology to turn the bit. Much of this drilling has occurred in shallow gas wells in Canada.

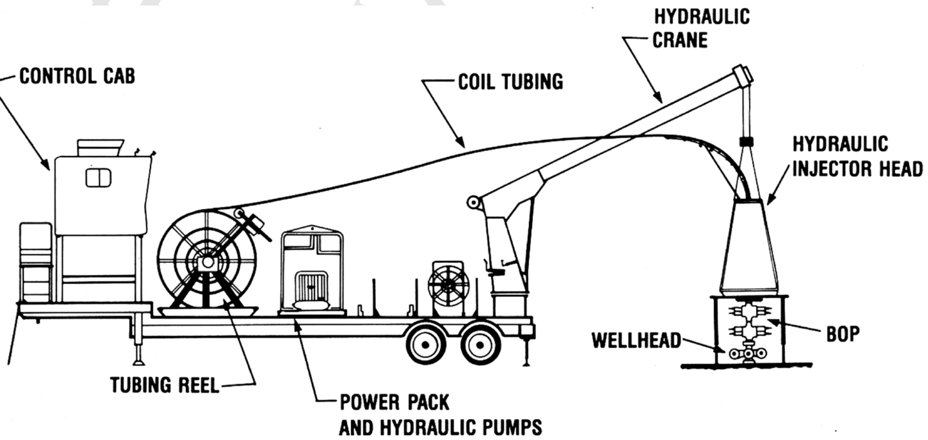

Figure 3.3 Typical coiled tubing unit. Photograph courtesy of and © Cudd Pressure Control, Inc.

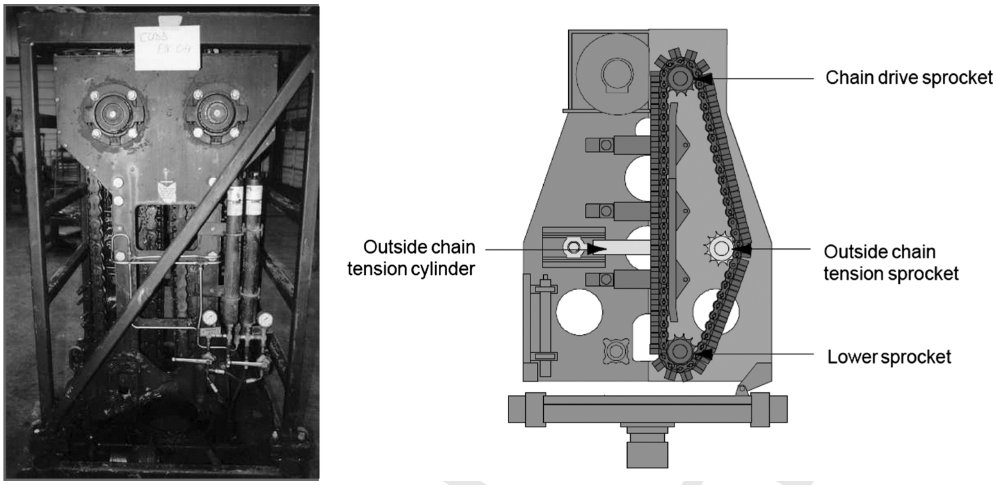

Figure 3.4 Coiled tubing injector head. Photograph courtesy of and © Cudd Pressure Control, Inc.

Directional coiled tubing drilling is complicated by the inability to rotate the coiled tubing itself, and place heavier pipe as desired in the coiled tubing string to facilitate optimal drilling weights and prevent buckling of the coiled tubing. The inability of the coiled tubing to rotate necessitates the use of a powered orienting device to rotate the directional assembly in the desired direction. This inability to rotate also increases the drag forces on the coiled tubing, limiting the reach and complexity of drilling paths. Currently, there are approximately 50 built coiled tubing drilling units, with most concentrated in Canada (Figure 3.5). These second-generation coiled tubing drilling rigs have been modified to allow coiled

Figure 3.5 Coiled tubing rig. Courtesy Technicoil.

Figure 3.6 Hybrid coiled tubing unit. Courtesy Technicoil.

tubing and jointed pipe to be used as desired, facilitating running casing and jointed production tubing (Figure 3.6).

A lot of research has been done on micro-drilling systems. A prototype built by the Los Alamos National Laboratory was tested at the RMOTC-operated Teapot Dome Field at NPR No. 3. The microdrilling rig includes the coiled tubing drilling unit, mud cleaning system, and a drilling-water truck.

3.2.2.2 Rotary Drilling Subsystems

Rotary drilling rigs use a string of pipe to connect the bit to the surface. The string can be rotated, in contrast to the coiled tubing systems. The rotary rig can be subdivided into subsystems. These subsystems consist of the power, hoisting, circulation, and rotary subsystems. A photograph of a modern rotary drilling rig is shown in Figure 3.7. This particular rig is a Helmerich and Payne Flex 4S Series rig drilling in Colorado.

3.2.2.2.1 Power Subsystem The energy needed for rotary drilling comes from the power subsystem. The main use of power in order of power requirements is for hoisting, fluid circulation, and rotation. Other power uses are for lighting, small transfer pumps, computers, and television sets, and the ubiquitous coffee pot. Most rigs need about 750–2000 kW.

The power for most drilling rigs on- or offshore is from diesel motors. The distribution of power is dependent on whether the rig is electric or direct drive. Diesel–electric rigs are similar to locomotives in that a diesel powers an AC generator. The power from the AC generator is sent through a “silicone control rectifier,”

Figure 3.7 Modern rotary drilling rig.

(SCR) and converted to DC power for distribution. This is because of the superior low-speed–high-torque capabilities of DC motors. These motors also have a wide speed range. The controls for a diesel–electric rig are relatively simple and flexible with a smooth power feed. These rigs also have plug-in portability. Even though these rigs have a very expensive initial cost, most newly built drilling rigs for hydrocarbon exploration are diesel–electric. There are a few new rigs using a new power distribution system that eliminates the SCR system, called AC synchronous drive rigs.

The other, older style of rig is the diesel–direct drive. Similarly to an automobile, the motors are physically connected to the power using devices such as the hoisting system or fluid circulation pumps. The diesel is directly connected using compounds (transmissions). These compounds consist of chains, belts, gears, and clutches. Shock and vibration are often a problem with these gears. There are a few that have hydraulic drives (automatic transmissions) and torque converters. These rigs tend to be smaller and have a far lower initial cost than diesel–electric rigs. Nonetheless, these rigs do not have the wide speed range of diesel–electric rigs and are forced to operate over a narrow range of outputs.

Power system performance is easily modeled. The power, P, can be found by using the following equation:

$$P = \omega T \tag{3.3}$$

where P = power, ω = angular velocity ($2\pi N$), N = revolutions per minute, and T = output torque. The heat energy input, Q, can be determined from the fuel use by

$$Q = w_f H \tag{3.4}$$

where w_f = fuel consumption rate and H = heating values of various fuels. The engine efficiency, E_t, is

$$E_t = \frac{P}{Q} \tag{3.5}$$

Factors that affect power are altitude (air density), temperature, humidity, and any accessory use.

3.2.2.2.2 **Hoisting Subsystem** The hoisting system is used to move the drill string in and out of the borehole and for lowering casing into the borehole. The hoisting system makes up the distinctive part of a drilling rig. It consists of a drawworks, block and tackle system, a mast, and a substructure. There are two common procedures for the hoisting subsystem, making connections and tripping. Making (and breaking) connections is the procedure for screwing or unscrewing the pipe that makes up a drill string or casing. Tripping is the procedure for pulling the drill string out of the hole to change a bit or bottom hole assembly and running the drill string back to bottom to continue drilling. Tripping is also used to remove the drill string from the borehole for other purposes such as running casing, measuring the borehole, or fixing something that has gone wrong.

The winch used for hoisting and braking power is called the drawworks. The drawworks stores the wireline that is part of the block and tackle system. The drawworks, the most power-hungry part of a drilling rig, is also used for making and breaking individual connections that make up a drill string or casing. The drawworks consists of a drum for the wireline and brakes. These breaks must be strong enough to hold whatever is being held. They are typically either of a band type or auxiliary breaks, such as hydraulic or electromagnetic, for long-duration use.

The mast (often called a derrick, although technically, that refers to a permanent structure, not portable), is used to provide the height needed to raise and lower the drill string or casing. Typically, it is high enough to remove one, two, or three sections of pipe, called joints, at a time. This greatly speeds up the tripping procedure if two or three joints can be pulled out and set back into the mast standing up. This is why these are called "stands." The mast must support the compressive load of the drill string and the weight of the various stands. In addition, the mast must handle any aerodynamic wind loading.

Under the mast is the rig floor, where most of the action takes place. Supporting the floor is the substructure. The substructure supports the mast and floor some distance above the ground. This space provides access to the well control equipment, various valves for controlling kicks. Typically, the deeper the well, the more pressure containment is needed. This means that the BOP equipment tends to be larger the deeper is the hole, which in turn means that the substructure must be taller and more robust to handle the heavier loads imposed upon it from the mast. In addition, on most rigs, the drawworks and rotary equipment also sit on the rig floor and, subsequently, the substructure must support that load also.

The block and tackle system consists of a crown block, traveling block, and the aforementioned drilling line. The crown block sits on the top of the mast and is stationary. It has multiple sheaves for running the drilling line. The traveling block has a corresponding number of sheaves and is free to travel up and down the mast on the drilling line. The drilling line running down to the drawworks is called the fast line and the drilling line running off the last sheave in the crown block is called the deadline. The deadline is anchored to the mast or substructure. The block and tackle system is use to provide a mechanical advantage for lifting. That mechanical advantage, M, can be determined by

$$M = \frac{W}{F_f} \tag{3.6}$$

where: W = load on traveling block and F_f = load on the drawworks (fast line tension). The ideal mechanical advantage, n, is

$$nF_f = W \tag{3.7}$$

Hence the ideal mechanical advantage is the same as the number of lines strung between the crown and traveling blocks. The input power, P_i, of a block and tackle system is

$$P_i = F_f V_f \tag{3.8}$$

where: V_f = velocity of the fast line. The power at the traveling block, often called the hook power, P_h, is

$$P_h = WV_b \tag{3.9}$$

where: V_b = velocity of the block. The block velocity is simply

$$V_b = \frac{V_f}{n} \tag{3.10}$$

For a frictionless system, the hoisting efficiency, E, is

$$E = \frac{P_h}{P_i} = \frac{WV_b}{F_f V_f} = \frac{\left(\frac{nF_f V_f}{n}\right)}{F_f V_f} = 1 \tag{3.11}$$

However, no system is frictionless, so the hoisting efficiency is always less than one. Rearranging Equation (3.11) allows for the determination of the fast line tension, the load going into the drawworks:

$$F_f = \frac{W}{nE} \tag{3.12}$$

The load on the mast is not simply the weight of the block and tackle and W. It also includes the forces from the deadline and fast lines. The mast load, F_d, is

$$F_d = W + F_f + F_s \tag{3.13}$$

where F_s is the dead line tension, which is

$$F_s = \frac{W}{n} \tag{3.14}$$

This can be noted by using basic statics and realizing that the load in the first sheave (dead line) is simply W/n (no movement hence no friction) and the load in the last sheave is the fast line tension, F_f. Substituting fast line and dead line equations we obtain the mast load:

$$F_d = W + F_f + F_s = W + \frac{W}{En} + \frac{W}{n} = W\left[1 + \left(\frac{1}{n}\right)\left(1 + \frac{1}{E}\right)\right] \tag{3.15}$$

For a mast or derrick that has four legs, it is important to note that the forces are not evenly distributed over the legs! Since the dead line is anchored along one leg, often called the A leg, it not only has one-quarter of the lifted weight, it also has all of the dead line tension. The last leg, called the B leg, does not have any hoisting loads from the fast and deadlines, so its loads are just one-quarter of the weight. The fast line tension is distributed over two legs that straddle the drawworks (often called the C and D legs), so they hold one-quarter of the lifted weight and half the tension in the fast line. These are shown in Equations (3.16–3.19).

To calculate the loads on the various legs is straight forward. Note that the procedure does not consider dynamic loads or aerodynamic loads. A mast will be designed based on the maximum values expected over the drilling of a well. These are:

$$F_A = W\left(\frac{1}{4} + \frac{1}{n}\right) \tag{3.16}$$

$$F_B = W\left(\frac{1}{4}\right) \tag{3.17}$$

$$F_C = W\left(\frac{1}{4} + \frac{1}{2En}\right) \tag{3.18}$$

$$F_D = W\left(\frac{1}{4} + \frac{1}{2En}\right) \tag{3.19}$$

Circulation Subsystem The circulation system is used to fill the borehole with fluid and circulate the fluid down the drill string and out of the annulus. The flow path starts at the rig pump and travels through the surface equipment on the rig under high pressure (Figure 3.8). The surface equipment is attached to a swivel hanging off of the traveling block using a flexible high-pressure hose called a rotary hose. The swivel is a piece of machinery that connects the drill string to the traveling block, allowing for drill string rotation and high-pressure fluid transfer.

The fluid flows down the drill string and exits the drill bit, typically through specifically sized nozzles. These nozzles are often sized to allow an optimum amount of pressure drop through them to maximize the hydraulic power or impact force expended on the bottom of the hole. This helps dislodge any cuttings, allowing the bit to penetrate a new surface. Sometimes in the bottom hole assembly there are pressure drops for small generators to power electronic equipment and

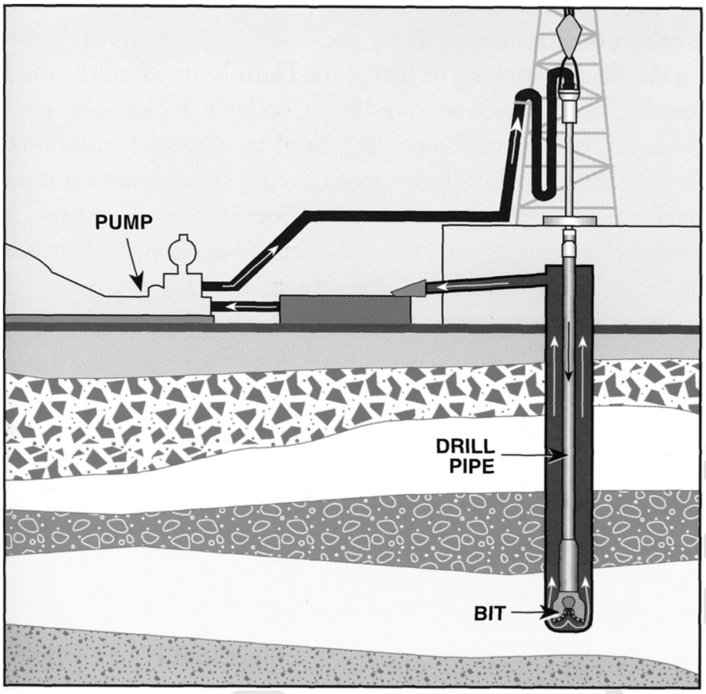

Figure 3.8 Fluid circulation system. Courtesy Petex.

Moineau-style motors for rotating the bit for directional control (which is discussed later in this section). These pressure drops are in addition to the nozzle pressure drops and friction pressure losses.

From the bottom of the borehole, the fluid travels up the annulus carrying the cuttings out of the borehole. The fluid flows out of the borehole through various screening and cuttings removal devices, called solids control equipment, to clean the fluid. The cleaned fluid is collected in pits where the fluid rheological and chemical properties are changed as needed and new mud is mixed. The pump picks up the fluid from the pits and pumped back down the borehole, starting the process again.

The pumps used on drilling rigs to pump liquids are of two types of positive displacement pumps: either a duplex or triplex type of piston pump. The advantages of these pumps are that they can move high solids-content fluids with abrasives and large particles, they are easy to operate and maintain and reliable, and they allow for a wide range of flow rates and pressures. For pneumatic fluids, compressors are used. The compressors are typically rotary screw (although some piston compressors are used) with booster piston compressors when higher pressures than a rotary screw compressor can put out are needed.

The first type of mud pump, as these are called, is the double-acting duplex pump. It has two cylinders with suction and discharge valves on both sides of the piston. The pump is double acting (it pumps on forward and backward strokes).

However, these pumps are not as volumetrically efficient (typically 85%) as other pumps in that they have many seals. It is an older style of pump.

The newer style of mud pump is the single-acting triplex pump. It has three cylinders and is single acting in that it has only a single suction and discharge valve on the open side of the piston. These pumps are more volumetrically efficient (typically 95%) and can be up to 100% efficient if a small centrifugal pump is pumping fluid into the piston, called precharging. These pumps are lighter and more compact and the mud pulsations from the pistons are lower in magnitude than the duplex pump.

The pump factor is the volumetric rate of the pump. The pump factor is the volume swept by all of the pistons. It is measured over the sweep of one piston. For a duplex pump, the pump factor, F_p, is

$$F_p = \frac{\pi}{2} L_{stroke}(2d^2_{liner} - d^2_{rod})E_v \tag{3.20}$$

and for a triplex

$$F_p = \frac{3\pi}{4} L_{stroke}(d^2_{liner})E_v \tag{3.21}$$

where L_{stroke} is the piston stroke length, d_{liner} is the piston diameter, d_{rod} is the diameter of the connecting rod, and E_v is the volumetric efficiency (1 for theoretical). To determine the flow rate, simply count the strokes in some time to obtain the stroke rate and then multiply that by volumetric rate. To determine E_v, calculate the theoretical value and determine an actual volume pumped. Divide the actual value by the theoretical values to obtain E_v.

The pump power requirement, P_h, is found by

$$P_h = Q\Delta P \tag{3.22}$$

where Q is the flow rate and ΔP is the pressure change. The piston diameter, called the liner size, controls the pressure and flow rate. Using large liners gives high flow rate but low pressures whereas small liners give low flow rates with high pressures.

The solids control system is used to remove undesirable solids, such as cuttings. The primary solids control equipment is the shale shaker, which is a vibrating screen just outside the exit of the borehole annulus. The screen size dictates the cuttings sizes removed. However, too small a screen can become plugged, so secondary solids control systems are used. These are either settling tanks, to give time for the cuttings to settle, or they are hydrocyclones. There are many different styles of hydrocyclones. The size of the hydrocyclone mechanisms dictate what size cuttings are trapped and what passes through. There is no perfect cuttings removal system.

3.2.2.2.3 **Rotary Subsystem** The main parts of the rotary system are the following:

- either a swivel, kelly, and rotary table or a top drive
- drill pipe
- bottom hole assembly (consisting primarily of drill collars)
- bit.

Figure 3.9 Kelly drive system.

The rotary system is the heart of the rotary drilling rig. As the name suggests, it rotates the bit. This is accomplished by spinning the entire drill string from the surface.

The swivel supports the weight of the drillstring, permits rotation, and connects the fluid pumping system to the drillstring. The swivel is attached to the hook of the traveling block, which is part of the hoisting system. The kelly is the first section of pipe below the swivel. The outside cross-section of the kelly is square or hexagonal to permit it to be gripped easily for turning. Torque is transmitted to the kelly through the kelly bushings that fit into the rotary table (Figure 3.9). The rotary table, driven by a rotary drive, imparts the torque to the drillstring through the kelly. The torque is transmitted through the drillstring to the bit.

A top drive is a newer system that incorporates the swivel mechanism and an electric or hydraulic motor that screws directly into the drill pipe. The majority of new rigs built for the oil industry use top drives. The motor rides up and down with the traveling block and ride on tracks mounted in the mast or derrick. These top drives also have mechanisms that allow for the tripping of pipe or even circulation while tripping pipe in and out of the hole (Eustes, 2007).

The drill string consists of drill pipe which is a lightweight pipe (relatively speaking, as they run from 2 3/8″ to 6 5/8 in in diameter). The drill pipe has large upsets on either end called tool joints. These add strength to the drill pipe for torsional and axial loading conditions. The drill pipe runs in length from 20 to 40 ft, typically 30 ft for API standard range 2 pipe. The major portion of the drillstring is composed of drillpipe. The drillpipe is a hot-rolled, pierced, seamless steel pipe that comes in various weights and material grades with strengths that range from 75 000 to 135 000 psi yield strength (API RP 7G, 1998).

The bottom section of the rotary drillstring is composed of drill collars and other specialized equipment. This section of the drillstring is called the bottom hole assembly. This is discussed further in the directional drilling section. The drill collars are thick-walled, heavy steel tubulars used to resist bending while in compression from adding weight to the bit for drilling. The buckling tendency of the relatively thin-walled drillpipe is too great to use it for this purpose (which would lead to significant fatigue issues).

The bottom hole assembly (BHA) consists primarily of the aforementioned drill collars. They resist bending as force is put on the bit [called weight on bit (WOB) in drilling][. In addition, stabilizers can be used towards the bottom of the BHA for directional control, such as increasing, decreasing, or holding the borehole angle. Furthermore, reamers can be used to open the borehole to larger diameters than the drill bit, or just to keep the borehole at the bit diameter. Also, Moineau-style downhole motors, called mud motors, can be used to keep the drill string stationary while still rotating the bit. Other downhole BHA equipment can be drilling operational sensors, called measurement-while-drilling (MWD), or formation sensors, called logging-while-drilling (LWD).

The final piece of rotational equipment is the drill bit. This is the business end of all drilling rigs and is discussed in the next section. More information on rotary rig calculations for power, hoisting, circulation and rotary subjects can be found in Bourgoyne *et al.* (1986) and Azar and Samuel (2007).

3.3 Penetrating the Material

The energy requirements for rock fracturing include many aspects: the drill must overcome the surface energy developed by fracturing; the strain energy must be overcome; strain wave propagation in both loading and unloading will require energy; finally, other energy sinks include rock crushing, fluid pressurization, and plastic deformation. To compare the different available drilling methods and the resulting drilling techniques in a normalized method, the specific drilling energy is introduced. The specific drilling energy is defined as the amount of energy required to remove a unit volume of rock.

In general, a distinction between four different kinds of rock destruction mechanisms can be made: melting and vaporization, thermal spalling, chemical reaction, and mechanical breakage. The most common drilling method is mechanical breakage. The primary reasons for the use of mechanical breakage are ease of application, advanced technical status, and environmental concerns with the other methods.

The energy demand to fracture rock is not a restricting factor in Earth-bound drilling. Most of the drilling rigs used on Earth have far more power available than is needed to drill. More on this energy usage was discussed in Chapter 2.

3.3.1 Basic Rock Destruction Mechanism

Rock excavation devices remove rock by four basic mechanisms, melting and vaporization, thermal spalling, mechanical breakage, and chemical reactions (Maurer, 1968, 1980). A catalog of drilling mechanisms and associated specific energies can be found in Table 3.1.

Table 3.1 Specific energy requirements for various drilling methods.

Drill method	Status	Removal mechanism	Specific energy ($J\,cm^{-3}$)	ROP maximum ($cm\,min^{-1}$)	Comments
Rotary	Field	Mechanical	200–500	14–85	Water-filled hole
Percussion	Field	Mechanical	250–400	50–80	Water-filled hole
Continuous penetrators	Field	Mechanical	—	—	High WOB required
Spark	Laboratory	Mechanical	200–400	35–140	Water-filled hole
Erosion	Laboratory	Mechanical	2000–4000	35–140	Water-filled hole
Explosive	Field	Mechanical	200–400	26–70	Water-filled hole
Forced flame	Field	Spalling	1500	28–56	Only @ spalling rock
Jet piercing	Field	Spalling	1500	9–18	Only @ spalling rock
Electric disintegration	Laboratory	Spalling	1500	9–14	Additional electric power
Pellet	Laboratory	Mechanical	200–400	4–14	Water-filled hole
Turbine	Field	Mechanical	400–1300	3–14	Water-filled hole
Plasma	Laboratory	Fusion	1500	2–3	Additional electric power
Electric arc	Laboratory	Fusion	1500	1–3	Additional electric power
High frequency	Laboratory	Spalling	1500	3–6	Just @ spalling rock
Electric heater	Laboratory	Fusion	5000	1–3	Additional electric power
Nuclear	Conceptual	Fusion	5000	1–3	Only 100 cm hole
Laser	Small holes	Spalling	1500	1–2	Only @ spalling rock
Electron beam	Small holes	Spalling	1500	1–2	Only @ spalling rock
Microwave	Laboratory	Spalling	1500	1–2	Only @ spalling rock
Induction	Laboratory	Spalling	1500	0.5–1	Only @ spalling rock
Ultrasonic	Laboratory	Mechanical	20 000	8-Apr	High energy use

3.3.1.1 Melting and Vaporization

The melting temperature of igneous rock ranges from 1100 to 1600 °C and limestone melts at 2600 °C. Lasers and electron beams produce sufficient power concentrations to melt and vaporize all types of rock. The high energy requirements of these rock-melting devices preclude their widespread use except for drilling small-diameter boreholes or for melting narrow kerfs in conjunction with mechanical cutters. Conceptually, these devices could also be used to melt narrow kerfs around large blocks of rock and remove the blocks intact. The total energy H required to fuse and vaporize rock is given by

$$H = c_s(T_m - T_i) + H_f + c_m(T_v - T_m) + H_v \tag{3.23}$$

where c_s is the mean specific heat of solid rock, T_m is the rock melting point, T_i is the initial temperature, H_f is the latent heat of fusion, c_m is the mean specific heat of liquid rock, T_v is the rock vaporization point, and H_v is the latent heat of vaporization.

It has been determined that most rocks melt at an average value between 4000 and 5000 J cm^{-3}. Furthermore, it is interesting that less energy is required to fuse strong, igneous rocks such as granite and basalt than to fuse sedimentary rocks such as sandstone and limestone. Considerably more energy is required to vaporize rock than is required to fuse them. For example, only 80 cal g^{-1} water is required to melt ice whereas an additional 640 cal g^{-1} is required to vaporize water.

3.3.1.2 Thermal Spalling

Heat creates thermal stresses that can fracture and degrade rock. These thermal stresses are produced by differential thermal expansion of the crystals and grains that constitute a rock. The main factors producing this differential thermal expansion are:

- high temperature gradients in the rock
- differences in thermal expansion coefficients among the different minerals
- phase changes in minerals
- removal of water of crystallization
- heating of liquid or gaseous inclusions
- chemical reactions causing breakdown in the mineral assemblage.

One of the most important mechanisms creating high thermal stresses in rock is the 0.82% volumetric expansion that quartz undergoes during its alpha-to-beta transition at 573 °C. When quartz experiences this phase change, high thermal stresses are induced in the minerals surrounding the quartz crystals because they constrain thermal expansion of the quartz. This constraint can produce high stresses. For example, if the thermal strain of an elastic material is constrained in only one direction, the stress (σ) on the constraints will be equal to

$$\sigma = \alpha Y \Delta T \tag{3.24}$$

where α is the linear coefficient of expansion, Y is the modulus of elasticity, and ΔT is the temperature change. Induced stresses are higher when thermal strains are constrained in more than one direction, for example, parallel to a heated surface.

3.3.1.3 **Mechanical Breakage**

Rocks are mechanically drilled by impact, abrasion, or erosion. These mechanisms induce tensile or shear stresses that exceed the rock strength and produce plastic yielding or brittle failure. Impact loads are produced by percussion tools, implosions, explosions, and underwater spark discharges. These impacts usually produce a zone of finely crushed rock directly beneath the area of impact. If sufficient force and energy are applied to the rock, fractures are initiated around this crushed zone. These fractures propagate along curved trajectories to the rock surface, breaking loose chips or fragments of rock.

Abrasion devices use hard, particulate materials such as diamond or tungsten carbide to abrade and remove rock. The particles usually move parallel to the rock surface, producing a crushed zone ahead of them and abrading a groove into the rock. If the depth of the cut is sufficient, fractures propagate along curved trajectories from the tip of the abrasive particle to the rock surface, forming chips ahead of the abrasive particle.

3.3.1.4 **Chemical Reactions**

A wide variety of chemicals can be used to dissolve rock. Highly reactive chemicals such as fluorine can drill rock at high rates. Safety problems and high chemical costs preclude the use of these chemicals for widespread drilling.

3.3.2 Specific Energy Comparison of Different Drilling Methods

A tabular comparison of drilling energies of different drilling methods is presented in this section. The listed power input was calculated by the various specific energy equations listed earlier. The drilling energy was calculated for drilling in hard to very hard rock, because the rocks on Mars are expected to be very high in compressive strength (up to 120 000 psi). On Earth, very hard rock usually means compressive strengths greater than 20 000 psi. The following drilling modes are presented and discussed: ultrasonic drilling, rotary drilling, and percussion drilling, with a short discussion of a continuous penetrator.

3.3.2.1 **Ultrasonic Drilling**

Ultrasonic tools are used commercially to drill and machine diamonds, ceramics, and other hard alloys. They can be used to drill rock. Ultrasonic drills use magnetostrictive or electrostrictive cores to vibrate emitters at frequencies of 20–30 kcycles s^{-1}. A magnetostrictive core consists of a nickel or permendur plate core with an electric winding through which a high-frequency current is passed. Under the action of the variable magnetic field, the core expands and contracts with an amplitude of several microns and a frequency equal to the current frequency. The amplitude of this vibration is amplified 10–100 times by using a resonant tapered horn between the magnetostrictive transducer and the cutting tool. The length of this horn plus the cutting tool is an exact multiple of the half-wavelength of the frequency. This creates a system of standing waves in the horn. The energy is supplied to the transducer and is transmitted through the tapered horn, thus magnifying the amplitude of vibration, which increases in proportion to the reduction in diameter.

The ultrasonic drilling tool removes rock by two mechanisms, cavitation and abrasion. Ultrasonic tools require an acoustic contact with the drilling material. In most cases, this is facilitated by water. In the water surrounding the emitter, cavities or bubbles form because of the transfer of energy from the emitter to the water. These cavities migrate towards the rock surface and collapse, forming high implosion pressures that microscopically crush the rock surface. Initially, the softer constituents are disintegrated, then micro-fractures develop around individual grains, and fragments spall from the surface. Cavitation dies out above pressures of 5–7 $kg\,cm^{-2}$; therefore, this mechanism would not be important in deep-well drilling.

Hard abrasives (such as boron carbide and carborundum) are usually introduced below the tool, producing a suspension of abrasive particles around the cutting tool. Turbulence produced by cavitation draws many of the abrasive grains beneath the cutting tool, which impacts and accelerates them towards the rock at high velocity. The resulting high-speed impacts crush and remove rock from the surface. High-speed movies made at the Acoustical Institute of the Academy of Sciences, USSR, established that this abrasive action is the primary cutting mechanism in ultrasonic drilling and that cavitation is relatively unimportant.

The cutting speed depends on the type of abrasive used. The drilling rate increases with increasing abrasive grain size, reaching a maximum when the grain size is slightly less than the peak-to-peak oscillation of the cutting tool. The drilling speed also increases with increased amplitude of vibration, because maximum particle velocity and maximum impact momentum are proportional to this amplitude.

With a 4 kW input, an ultrasonic drilling device is able to drill 5–8 cm boreholes, removing a maximum of 10 $cm^3\,min^{-1}$. This corresponds to a specific energy of 24 000 $J\,cm^{-3}$ based on input energy. The limiting lateral dimension of the ultrasonic cutting tool is about one quarter wavelength of the horn that couples the transducer to the cutting tool. At the lowest ultrasonic frequency of 20 $kcycles\,s^{-1}$, the maximum cutting tool diameter is about 6.5 cm.

The advantages of ultrasonic drilling are a high rate of penetration in hard rocks, no dulling, and small borehole size. The disadvantages are high energy requirements, low rate of penetration in soft rocks, and the need for an acoustic connection (fluid).

3.3.2.2 **Rotary Drilling**

Rotary drilling, introduced about 1880, is the most widely used method of drilling wells today. Most industries that drill into the surface of the Earth, petroleum, geothermal, mining, water, and environmental, use the rotary method. The rotary system includes all of the equipment used to achieve bit rotation.

One of the most important parts of the rotary system is the drill bit, which does the actual drilling work. Extremely wide varieties of bits are manufactured for different situations encountered during rotary drilling operations. Rotary drilling bits are usually classified according to their design as drag bits and rolling cutter bits.

3.3.2.2.1 **Drag Bits** All drag bits consist of fixed cutter blades that are integral with the body of the bit and rotate as a unit with the drillstring. The design feature of the drag bit includes the number and shape of the cutting blades or diamond stones and the metallurgy of the bit and cutting element (Simon, 1958). Drag bits drill by physically plowing cuttings from the bottom of the borehole much as a farmer's plow cuts a furrow in the soil (Appl and Rowley, 1968).

Drag bits include the following kinds of bits:

- steel cutters
- diamond bits
- polycrystalline diamond compact (PDC).

Steel cutters style bits are some of the oldest style of bits designed. These style bits are often called "fishtail" bits from their appearance. They rapidly dull in any formation greater in strength than unconsolidated sands. Because of that, and the fact there are much better bits available, they are infrequently used today.

Diamond bits are bits that have diamonds of various sizes embedded on the surface of the bit within a tungsten carbide matrix. For surface set diamond bits, the assumed principal mode of material removal is the plowing action. The best material to be rotary drilled by a diamond bit is approximated by a rigid plastic Coulomb-type material. Other materials do not cut as well. A very important item in surface set diamond bits is the interaction of the drilling fluid with the mechanics of the cutting action.

A PDC bit is also a diamond style bit. However, the diamond is grown synthetically on to the round face of a tungsten carbide cylinder. This cylinder, called a cutter, is either held in place on the face of the bit by a steel post or embedded in a tungsten carbide matrix. In comparison with the surface set diamond bit, the PDC bit drills by cutting a formation in shear (Hycalog, 1994).

A PDC consists of a tungsten carbide cylinder with a diamond grit coating on one end. The enabling technology was to develop a multiple crystalline growth of diamond crystals on to and leached into the tungsten carbide cylinder. This is accomplished by subjecting the diamond grit deposited on the cylinder to 13 700 mPa (2×10^6 psi) and 1500 °C (2730 °F) (Besson *et al.*, 2001), fusing the material on to the cylinder in a polycrystalline growth. Since the PDC bit is created in a mold with the compacts positioned prior to pouring of the metal substrate, the design of the PDC bit can be almost unlimited in shape and size.

PDC bits cut rock by causing a rock failure along the shear planes of the rock face. This is in contrast to the typical crushing/gouging action of a rolling cutter drill bit. The first PDC bits were only useable in soft to very soft rock formations. Today, PDC bits are used virtually everywhere that standard rolling cone drill bits are used in up to medium-hard formations. In fact, the PDC has about a 50% market share in the Rocky Mountain region.

Another type of drag style drill bit entering the market is the impregnated diamond drill bit. This type of drill bit is designed for ultra-hard, abrasive rock formations. It has been in existence from the 1800s but the technology to insure wear resistance is finally catching up with the times. The bit consists of a diamond grit that is mixed with a tungsten carbide substrate and molded into intricate shapes as dictated by the bit design. The wear resistance of impregnated bits is outstanding in abrasive formations.

A forward force is applied to the cutter from the application of force on the bit, and a side force is applied to the cutter from the application of the torque necessary to turn the bit. The result of these two forces defines the plane of thrust of the cutter or wedge. The cuttings are sheared off in a plane at an initial angle to the plane of thrust that is dependent on the properties of the rock. The depth of the cut is controlled by the plane of thrust and is selected based on the strength of the rock and the radius to the cut. The depth of the cut is often expressed in terms of the bottom-cutting angle, α_b. This angle is a function of the desired cutter penetration per revolution, L_p, and the diameter of the borehole, D:

$$\tan \alpha_b = \frac{L_p}{\pi D} \tag{3.25}$$

The Mohr failure criterion can be applied to relate rock strength measured in simple compression tests to the rotary drilling process. The Mohr criterion states that yielding or fracturing should occur when the shear stress exceeds the sum of the cohesive resistance of the material, c, and the frictional resistance of the slip planes or fracture plane. The Mohr criterion is stated mathematically as

$$\tau = \pm(c + \sigma_n \tan \theta) \tag{3.26}$$

where τ is the failure shear stress, c is the material cohesive resistance, σ_n is the normal stress at the failure plane, and θ is the internal friction angle.

According to this equation, the shear strength increases with increasing normal stress on the failure plane. As shown in Figure 3.10, Equation (3.26) is the equation of a line that is tangential to Mohr's circle in two compression tests made at different levels of confining pressure. To understand the use of Mohr's criterion, consider a

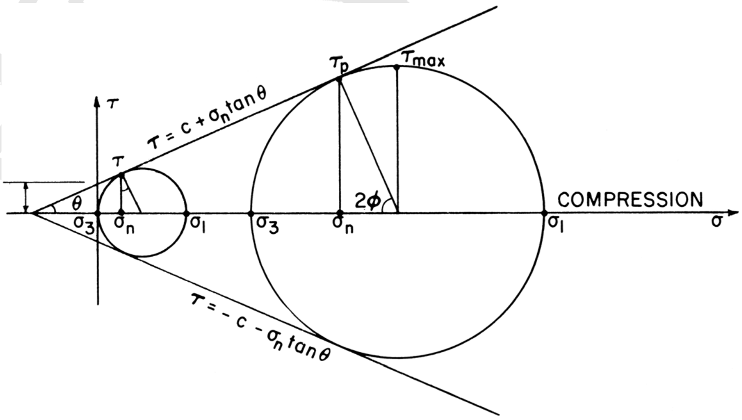

Figure 3.10 Mohr–Coulomb failure criterion (Bourgoyne *et al.*, 1986).

rock sample to fail along a plane, when loaded under a compressive force F and a confining pressure p. The compressive strength σ_1 is given by

$$\sigma_1 = \frac{F}{\pi r^2} \tag{3.27}$$

and the confining stress is given by

$$\sigma_3 = p \tag{3.28}$$

The advantages of the Mohr–Coulomb failure model are that deviations of the criterion from test results are not prohibitive considering the simplicity of the criterion, and the combined criterion provides a partial explanation concerning the tensile and compressive (shear slip) modes of failure. The chief limitations of the Mohr–Coulomb model are that there is no influence of the intermediate principal stress, the meridians are straight lines, and the strength parameter, ϕ, does not change with confining pressure. This approximation becomes poorer with increasing hydrostatic pressure. In addition, the failure surface is not a smooth surface, but has corners which appear as singularities in the mathematical treatment.

The Mohr–Coulomb relation becomes inaccurate when the failure envelope becomes markedly curved. Nonlinear shear strength envelopes have been reported for many rock types and soils. The most common relation used for soil, rock infill, and jointed rock is the power curve relation, since it best represents the reported data and is a simple mathematical relation (Desai and Siriwardane, 1984). When the power curve relation is applied to shear strength, it is as follows:

$$\tau = A\sigma^b \tag{3.29}$$

where τ is the shear stress at failure, σ is the effective normal shear plane stress, and A and b are material properties. Compared with other linear relations, this equation is relatively simple. These two material properties, A and b, can be calculated from the test data (Hycalog, 1994). These two properties remain constant over a range of effective stresses.

One of the criteria for this model is that a zero intercept is a requirement; consequently, no cohesion exists at zero effective stress. This is not valid for cemented and bonded soils because these materials can sustain significant tensions (Chen and Saleeb, 1982).

The parameters A and b have been found by drawing a hand-fitted power curve to the Mohr circle. The procedure presented by Perry (1992) for fitting a power curve to Mohr's circle is based on the least sum of squares method. This method is reasonably accurate. In addition, Hock and Brown (1982) derived a modified power-law failure criterion for rock in varying states of fracture.

3.3.2.2.2 **Rolling Cutter Bits** Rolling cutter bits have one or more cones on which the cutting elements are either cut or pressed. The cones rotate about their own axis, which is approximately perpendicular to the bit rotation axis. The cones roll about the bottom of the borehole as the bit rotates. The three-cone rolling cutter bit is by far the most common bit type currently used in rotary drilling operations. This general bit type is available with a large variety of cutter designs and bearing types and is suited for a variety of formation characteristics.

The drilling action of a rolling cutter bit depends to some extent on the offset of the cones. The offset of the bit, sometimes called skew, is a measure of the angle between the cone axis and the bit rotation axis as measured perpendicular to the bit rotation axis. Offsetting often causes the cone to stop rotating periodically as the bit is turned. This causes the cone teeth to scrape the bottom of the borehole somewhat like a drag bit. This action tends to increase drilling speed in most formation types. However, it also promotes faster cutter wear in abrasive formations. The cone offset angle varies from about 4° for bits used in soft formations to zero for bits used in very hard formations.

The two primary types used are milled tooth cutters and tungsten carbide insert cutters (Bourgoyne *et al.*, 1986). The milled tooth cutters are manufactured by milling the teeth on a steel cone. A tungsten carbide insert bit is manufactured by pressing a tungsten carbide insert into an accurately machined hole in the cone.

As a load is applied to a cutter, the constant pressure beneath the cutter increases until it exceeds the crushing strength of the rock. A wedge of finely powdered rock is formed beneath the cutter. As the force on the cutter increases, the material in the wedge compresses and exerts high lateral forces on the rock surrounding the wedge. Eventually, the shear stress exceeds the shear strength of the rock and the rock fractures. These fractures propagate along a maximum shear surface, which intersect the direction of the principal stresses at a nearly constant angle as predicted by the Mohr failure criteria. The force at which fracturing begins is called threshold force. As the force on the cutter increases above the threshold value, subsequent fracturing occurs in the region above the initial fracture, forming a zone of broken rock. The cutter then moves forward until it reaches the bottom of the crater, and the process is repeated.

With a negative differential pressure between the borehole and formation (higher formation pressure than borehole pressure), the cuttings formed in the zone of broken rock are ejected easily from the crater. At positive differential pressures, the downward pressure from the borehole with subsequent frictional forces between the rock fragments limits ejection of the fragments. This is called the "chip hold-down pressure" and explains why "underbalanced drilling" is faster than "overbalanced drilling."

As the force on the cutter is increased, displacement takes place along fracture planes parallel to the initial fracture. This gives the appearance of plastic deformation, and craters formed in this manner are called pseudoplastic craters. The drilling action of rolling cutter bits designed with a large offset for drilling soft, plastic formations is considerably more complex than the simple crushing action that results when no offset is used. Since each cone alternately rolls and drags, considerable wedging and twisting action is present.

The mechanical output to the rock for conventional drilling is proportional to the torque and the rotation rate required at the bit. Less mechanical power is developed in rocks with greater strength, which leads to a more rapid decrease in rate of penetration (ROP) than in inverse proportion to the drilling strength

(Simon, 1958). The fact that only a fraction of the power of the rotary table can be transferred into mechanical power output at the rock is one of the main limitations of the rotary drilling process. Advances made in rotary drilling have consisted primarily of improvements in mechanical design.

The advantages of rotary drilling are many. It is adaptable to any type of formation. In addition, one can drill underbalanced with a significant increase in rate of penetration. There are also a wide range of bit styles and sizes. Finally, rotary drilling is the most popular and widely used drilling method available. The disadvantages of rotary drilling include dulling and subsequent replacement of the bit. Rotary bits also need to have enough force applied to overcome the threshold pressure needed to start drilling.

3.3.2.3 Percussion Drilling

Percussion drilling is an ancient drilling technique and is used in areas where the compressive rock strength is extremely high, such as in hard-rock mining operations (Hustrulid and Fairhurst, 1971). Percussion drilling is a process in which repeated impacts are applied to the rock surface through a pointed tool. The technique has been improved by the development of the percussion–rotary technique, in which positive rotation of the tool, together with a high static thrust, have been superimposed on the basic percussion action. Howe has proposed the principle of a continuous penetrator, a type of percussion drill, similar to the approach of the subsurface explorer, for drilling porous rock or unconsolidated material (R.J. Howe and W.C. Maurer, Esso Production Research, Houston, TX, personal communications, 1963).

The penetrator crushes the rock and displaces it into a zone of crushed rock surrounding the borehole. The penetrator would obviate pulling drill pipe to the surface to replace worn bits, and it would require no circulating fluid to remove the cuttings. The high forces required for penetration would be produced by the weight of drill collars, by impact loads, or by wall anchors that grip the borehole walls and hydraulically load the penetrator. Well anchors of this type have been successfully tested in oil wells (Maurer, 1980).

The penetrator would produce a zone of crushed rock surrounding the borehole; this zone would have a radius r equal to (Maurer, 1980):

$$r = r_0\sqrt{\left(\frac{1-\phi_c}{\phi_R-\phi_c}\right)} \tag{3.30}$$

where r_0 is the radius of penetrator, ϕ_R is the rock porosity, and ϕ_c is the crushed rock porosity.

In general, the porosity of the solid rock would be much greater than that of the crushed zone ($\phi \gg \phi_c$) and ϕ_c would be much less than unity, in which case the radius equation for the crushed zone reduces to

$$r \approx \frac{r_0}{\sqrt{\phi_R}} \tag{3.31}$$

This crushed zone can be very large in rocks with low porosity. For example, the radius of a crushed zone in a rock with 5% porosity would be more than four times the radius of the penetrator.

In tests performed by Maurer, 0.7 cm diameter projectiles shot into porous sandstone rock had an average deceleration force of 29 411 N. Static tests and impact tests in unconsolidated material indicated that most of this force was directed toward overcoming the strength of the rock. Only a minor part of the force was from the inertia of the crushed rock ahead of the projectile. The force on a penetrator should be proportional to the projected cross section area, which indicates that forces on the order of (9–49) $\times 10^6$ N would be required on a 20 cm diameter penetrator in porous sandstone. These high forces appear to make the continuous penetrator impractical for drilling medium- or high-strength rock.

Similar projectile guns have been tested on a larger scale for excavating tunnels in rock. Initial results were encouraging, but as the tunnel progressed; the poor ability of this approach to kerf the tunnel fully became apparent. The excavation became narrower and could not be widened by the projectiles alone.

Since the penetrator produces a zone of crushed rock, it should be possible to use a smaller penetrator and to ream out mechanically or hydraulically the crushed zone surrounding the borehole. Equation (3.31) states that a 5 cm penetrator would produce a crushed zone large enough to be reamed out to a 20 cm diameter borehole in a rock with 5% porosity. This would reduce the average force required on the penetrator in sandstone from about 29×10^6 to about 1.8×10^6 N. In very weak rocks with high porosities, these forces would be considerably lower. Because of the high force requirement, the continuous penetrator appears to have potential application only in weak, highly porous rocks or in unconsolidated material.

The advantages of the continuous penetrator are that no drilling fluids are required, no drillstring is required, and a high rate of penetration in unconsolidated formations is possible. The disadvantages are a low rate of penetration in hard rocks, a high dulling rate, a potentially enlarged borehole diameter, and difficulty in transporting cuttings from under the tool.

Percussion drilling machines have been extensively used for drilling in mining for centuries. It is only in recent times that the mechanics of the percussion system and the efficiency of energy transfer from piston into the rock have been studied (Lundberg, 1973). In percussion drilling, a piston impacts a drill steel, transferring its momentum and energy to the steel in the form of a stress wave. The efficiency of energy transfer in this process has been shown experimentally to be nearly 100%, provided that

$$t_{\mathrm{sw}} \leq \frac{2L_{\mathrm{s}}}{v_{\mathrm{s}}} \tag{3.32}$$

where t_{sw} is the stress wave time duration, v_{s} is the longitudinal wave propagation speed, and L_{s} is the drill steel length. For a typical drilling machine, this requirement is satisfied if L_{s} is greater than 1.2 m. The fact that the observed experimental value is somewhat less is probably due to hysteretic-type losses in the piston and drill steel and energy losses from flexural wave generation.

The stress wave generated by the piston in the drill steel travels to the bit–rock interface. Part of the energy in the wave goes into the rock fracturing and part is reflected. Although some energy must be transmitted elastically to the rock, it was shown that this is negligible compared with that in rock fracturing (Simon, 1964).

To ensure that the bit and rock are in contact at the time of arrival of the first incident wave at the bit–rock interface, an axial thrust force must be applied. Low thrust results in overtravel or free rotation of the bit. If the bit is off the bottom, the energy applied during this event is ineffective in causing rock fracturing or penetration. Higher thrusts reduce free rotation but, because rotation or indexing takes place during the up- or back-stroke of the piston, increased bit pressure increases the indexing torque level. As thrust continues to increase, a point will be reached where the indexing torque will cause the drill to stall. Each drill will have an optimum thrust that will give a maximum penetration rate. It was observed that after a certain thrust is applied, any further increase results in no significant increase or even a slight decrease in penetration rate (Bruce *et al.*, 1969).

The rock strength strongly affects the ROP: the stronger the rock, the slower is the ROP. Experiments performed by Hustrulid and Fairhurst (1971) showed that a variable displacement in hard rocks occurs at rather low force levels (<5000 lbf). Further, it was shown that the energy transfer to the rock depends on the rod geometry and that it takes more energy to remove a given volume of rock dynamically than statically. This phenomenon can be explained by the different values of the rate of loading. Rock is stronger under high loading rates.

A strong influence on the volume to energy ratio is the indexing angle (angle of rotation), as shown by tests performed by Drilling Research Inc. (Bruce *et al.*, 1969). Following the results of these tests, the optimum indexing angles were determined experimentally and are approximately related to the impact energy by the following equation:

$$\frac{I_1}{I_2} = \frac{E_1}{E_2} \tag{3.33}$$

where I is the indexing angle and E is the impact work.

Other studies and experiments performed by Hartman (1959) using a 120° wedge bit with a smooth surface led to the following conclusions:

- An optimum indexing angle exists which is energy dependent.
- The minimum E_v for the bit–rock combination is independent of energy.
- The optimum indexing angle lies between 30° and 45°.

When optimizing indexing relations, the bit diameter appears to be a more important factor than rock type and bit type. However, bit shape is nevertheless very important.

Hartman also stated that a slightly rounded wedge of about 90°-included angle should be the preferred shape. In general, a conical shape of the bit should be preferred to a square shape (Pang *et al.*, 1986). If indexing is applied, the bit shape becomes even more important. Indexing can reduce the bit thrust for maintaining the same ROP by applying a patterned bit (for example, a four-point star shape).

The conclusions that can be drawn from the results stated above are the following:

- It is very important to maintain a thrust force that is large enough to ensure contact of the bit with the rock surface at all times.
- No indexing of the bit would lead to a lower or no penetration.
- The bit shape has a major impact on the percussion penetration rate.

3.4 Cuttings Transport and Disposal

3.4.1 Cuttings Transport from Under a Bit in Terrestrial Operations

In order to penetrate rock, the rock material that has already been fragmented, called cuttings, must be removed from under the bit in order to access new rock to penetrate. This is called bit cleaning in most drilling literature. The re-penetration of cuttings, a process called regrinding, is a source of significant drilling inefficiency, and is manifested by a decrease in penetration rate with no decrease in applied power. Energy-efficient drilling requires that regrinding be minimized.

There are two methods to remove the cuttings from beneath a bit: mechanically and with fluids. Mechanical methods remove the cuttings by physically pushing the cuttings from under the bit with an auger/shovel mechanism. This mechanism is subject to wear and friction problems. Fluid methods use either a liquid or gas flowing across the bit face, either from inside the bit to outside or vice versa (reverse circulation), to pick up and carry the cuttings from under the bit. The flow rate and face flow pattern are critical to the efficiency of fluid cleaning. The use of fluids is the preferred method of bit cleaning for anything other than the shallowest of wells.

In 1965, M. Grant Bingham published a method for determining the efficiency of drilling. He performed many hundreds of field and laboratory tests to determine that there are four general ways that a bit responds to operational parameters. He developed the drilling efficiency diagram (Figure 3.11) (Mitchell, 1992). On the abscissa, he normalized the WOB by dividing by the bit diameter (D). On the ordinate, he normalized the penetration per revolution by dividing the ROP by the rotary speed (N). This is the volume of rock removed per revolution of the bit. Higher values mean faster penetration. However, more WOB means faster wear. Therefore, points that are high and to the left on the diagram indicate more efficient drilling and longer lasting bits.

A typical equation used in the previous diagram is

$$\frac{\mathrm{ROP}}{N} = k\left(\frac{\mathrm{WOB}}{D}\right)^{a} \tag{3.34}$$

According to Maurer, for maximum performance of a bit, the exponent $a = 2$. If the bit cleaning is not complete, the performance curve will bend out at the point where incomplete cleaning occurs. The lower limit line is for a lower value of the exponent,

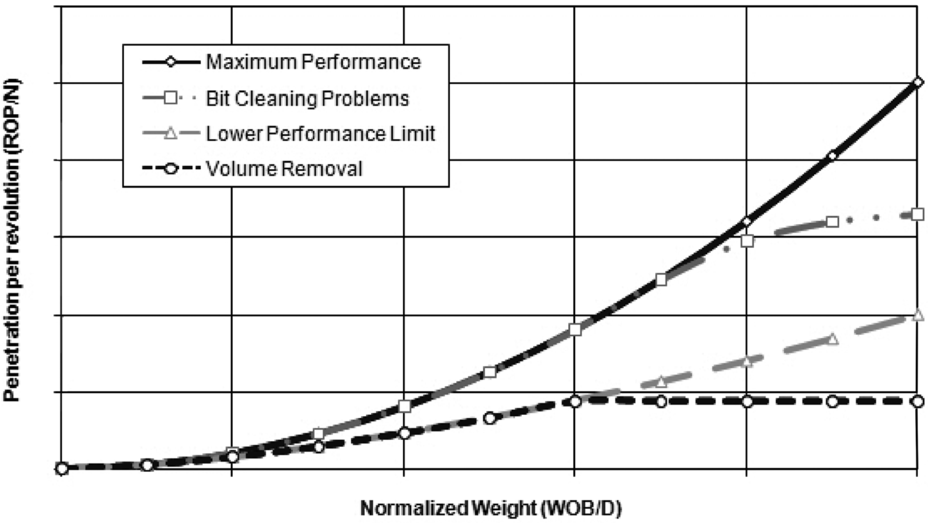

Figure 3.11 Bingham drilling efficiency generic diagram.

around one. This means that the drilling operational parameters and the drilling fluids have not been optimized for maximum performance. The volume removal line indicates that the bit has a total lack of bottom hole cleaning, often the result of bit balling. Bit balling is when the cuttings stick to the bit and interfere with the teeth/buttons penetrating new formation.

Optimal bottom hole cleaning occurs when 100% of the cuttings are removed from between the bit and the bottom of the hole. If the bottom hole cleaning values are greater than 100%, then this leads to an inefficient application of drilling energy. For a given rock and bit and a constant WOB and rotary speed, the ROP will be dependent on the bottom hole cleaning efficiency. Beyond 100% cleaning, the ROP stays relatively constant, assuming that there are no impact force effects. If there are impact force effects, then the hydraulic impact force is making penetration and it too must include cleaning effects.

The Bingham drilling efficiency diagram can be used to determine the point at which 100% cleaning takes places. The flow rate at which this occurs is the point for the minimum fluid flow rate for optimum bit cleaning. The point on the diagram where the drilling curve has an inflection shows where cleaning constraints are affecting penetration rates.

3.4.2
Cuttings Transport Beyond the Bit

The cuttings created under the bit must be transported away from the bit for it to advance into the sediment or rock. In the special case of a self-advancing mole, this can happen through either cuttings disposal at the bit (as in sonic drilling) or direct motion of the cuttings past the body of the drill system for disposal behind or at the side of the drill system, temporary storage along the wall of the borehole while the drill system itself passes by, or (the most likely scenario) a combination of all three mechanisms. In fact, the relative contribution of these three mechanisms will be controlled by the properties of the material through which the mole is advancing and thus will change throughout its working life. For most terrestrial drills (except sonic drills), the cuttings are removed from the hole entirely; this process is dealt with in a subsequent section.

The rock fragments and regolith particles constitute a system of macroscopic particles that interact almost entirely through the forces at their contact points (Jaeger, 1997). The body forces (weight) of individual chips are negligible in comparison with these contact forces. This class of material acts sometimes as solids, sometimes as fluids, often as strangely intermediate materials that defy standard description and confound performance prediction. In many situations, a positive feedback mechanism develops that leads to the formation of high-density particle clusters. Inside these high-density regions, the granular material acts as a solid, but outside them, the material acts as a liquid; the boundaries change in response to non-intuitive boundary and forcing conditions. This situation is characteristic of most low-speed or vibration-induced particle flows. Motion is concentrated in shear bands on the order of a few to several tens of particles in width. Compaction of granular material is essentially the same collection of phenomena as convection, but without the particle circulation components. The local distribution of forces in a granular material is extremely difficult to predict. Contact forces are distributed randomly, not evenly, among the multiple grain contacts that any single grain experiences. This leads to the formation of irregular "force chains."

Convection in dry granular materials is a circulatory, macroscopic flow pattern that arises when constrained collections of grains are shaken or vibrated. Its study forms the theoretical basis for size classification in fragmented materials such as ore processing streams. Granular convection in a drill system is most obvious during advance through loosely packed materials. In this instance, the drill system body itself can be thought of as a large, acicular particle in a bed of much smaller, equidimensional particles. Laboratory studies of long cylinders filled with round grains of consistent size show that wall friction is a controlling feature during discrete tapping events as well as during continuous vibration.

According to Knight *et al.* (1996), the depth of the convective region scales with the amplitude of the forcing function, and the typical time for a convective roll increases exponentially with increasing driving frequency (for fixed acceleration) and diverges as a power law as the ratio of applied peak acceleration to gravity approaches one (for fixed frequency). This means that convection is essentially stopped by vibrating a system at high frequencies (>50 Hz) and small amplitudes.

Ultra-low-power drilling systems can cross over from static to rapid flow states repeatedly; unfortunately the transition between these two is very difficult to handle in a predictive sense. This transition is a function of particle density, and involves passage through a complex sequence of metastable particle configurations. The particle density increases enough that chips get in each other's way, slowing the system response. Groups of entire particle clusters, instead of individual particles, set the time scale. This causes the system to jam, trapped far from any steady state, and imprints a memory of its preparation history. This in turn can lead to highly irreversible and hysteretic behavior in many circumstances. Understanding of how (and what) system parameters control this behavior is incomplete at best.

3.4.2.1 **Complete Cuttings Removal**

Once the cuttings have been flushed from under the bit, they must be removed from the hole. Again, two methods are used: mechanical, fluid, or both. Mechanical means are typically augers.

For drilling fluids, this cuttings removal is one of the primary tasks. If there is not enough transport, the cuttings can literally rain out around the borehole drilling equipment, leading to equipment sticking or even hole loss. Not only that, but upon cessation of fluid circulation, either the cuttings must be out of the borehole or the fluid must support them from falling. Inadequate borehole cleaning can lead to many other problems, such as high torque and drag for rotating equipment, increased bit wear, slow ROP, and potential formation fracturing and loss of fluid to formation.

There are five factors that affect cuttings transport: gravity, viscous drag, buoyancy, impact from other cuttings, and sidewall friction. In vertical holes, the viscous drag force, which is related to the viscosity and velocity of the fluid, on the cuttings from the fluid is collinear with the gravity and buoyancy forces. In non-vertical holes, this is not true and leads to cuttings bed deposits on the side of the borehole. Impact from other cuttings tends to break the cuttings into smaller pieces. In many ways, this makes cuttings transport easier. However, smaller cuttings mean that it is more difficult to remove those same cuttings from the fluid at the surface. Basically, cuttings transport out of a borehole boils down to two things: velocity and viscosity.

A useful concept in cuttings transport is the transport ratio (Sifferman *et al.*, 1974). This is the ratio of the cuttings slip velocity (the settling velocity) as it falls to the fluid velocity:

$$R_t = \frac{V_f - V_s}{V_f} \tag{3.35}$$

where: V_f is the fluid velocity, V_s is the cuttings slip velocity, and R_t is the transport ratio. Clearly, if $R_t = 1$, there is no slippage of the cutting with respect to the fluid. This is as good as it can get. If $R_t = 0$, the cuttings are falling as fast as the fluid is flowing and the cutting is just "hanging there." If R_t is negative, the cuttings are piling up in the borehole, and serious difficulties in continuing to drill will occur.

There are many factors that affect the transport ratio. The fluid's rheological properties are certainly a large variable. In addition, the fluid velocity and its flow regime have a large affect. However, other factors include the cuttings sizes, density, and shapes, borehole inclination and cuttings bed development, rotational speed if the drilling system is rotational, the eccentricity of the drilling system relative to the borehole, and the drilling ROP.

A simple volume fraction of cuttings in a borehole for steady state conditions can be found by the following:

$$V_{fc} = \frac{\mathrm{ROP} \times H^2}{Q R_t} \tag{3.36}$$

where V_{fc} is the volume fraction of cuttings in the borehole, H is the borehole diameter, Q is the flow rate, and R_t is the aforementioned transport ratio. Typically, for rotary drilling applications on Earth, if V_{fc} is larger than 5%, then difficulties with drilling can be expected (Azar and Samuel, 2007). Other, more complex, equations for cuttings volume fraction calculations are available for analysis in Mitchell (1995), Azar and Samuel (2007) and Bourgoyne *et al.* (1986).

A factor that should not be overlooked is the average annual density of the fluid. With the increase in cuttings, since the cuttings are typically denser that the fluid (not true in water-ice), then the overall density of the fluid increases with increase in cuttings volume fraction. This could lead to loss of fluid in the borehole (called lost circulation).

3.4.2.2 **Hydraulic Issues**

In the previous sections, it was assumed that a fluid was used to remove the cuttings. Because this fluid must be in motion, there is a dynamic hydraulic pressure associated with moving the fluid. This is true whether the fluid is liquid, pneumatic, or a combination of the two. There are many texts covering the calculation of these pressure effects. These include the already mentioned Mitchell (1995), Azar and Samuel (2007), and Bourgoyne *et al.* (1986), and also includes good references on pneumatic drilling by Lyons (2000) and McLennan *et al.* (1997). One thing to keep in mind is that adding the dynamic hydraulic pressure effects will increase the pressure within the borehole. This is called the equivalent circulating density (ECD) in the drilling industry and will exacerbate the potential lost circulation problem.

3.4.3
Cuttings Removal *In Situ*

If the soil particles and rock fragments created during the advance of a bit cannot be removed by the standard terrestrial practice of removal, then they must be handled downhole. When solid or even well-compacted unconsolidated materials are fragmented, they bulk, occupying greater volume than in the original state. Successful operation of a drill requires that the bulking be counteracted by one or both of these mechanisms:

- recompaction of the cuttings
- particle size reduction (crushing)
- particle packing to reduce pore volume
- creation of additional disposal volume by:
  - compaction of *in situ* porous material in the immediate vicinity of the bore
  - fracturing of *in situ* material in the immediate vicinity, followed by transport and compaction of particles to the fracture volume.

This section discusses approaches from the empirical to the theoretical from mining, mineral processing, geological, and civil engineering that apply to these areas.

3.4.4
Recompaction of Cuttings

Recompaction is accomplished by a combination of particle size reduction and particle packing. Particle size reduction occurs through fracture of the solid material, whereas packing occurs when the particles are moved, usually by fluidization through addition of liquid or by vibration.

3.4.4.1 Crushing

The size of a particle is reduced by crushing it. The physics of the process depend on how force is applied to the particle (Prasher, 1987). The relative proportions of the four possible comminution mechanisms (impact, compression, shear, and attrition) control the size distribution of the resulting fragments, which in turn affects the degree of recompaction that can be achieved. It is not yet possible to determine fully which mechanism is dominant in the various forms of comminution (crushing and grinding) in use today, but the results of each mechanism have been studied thoroughly. All materials have a critical particle size below which material behavior changes from brittle elastic to completely plastic. Below that size, further comminution changes only particle shape, not size. Both deformation and comminution require energy.

The basic relationships between applied energy and cuttings production are complex because solids exist due a dynamic equilibrium of the cohesive bonds between atoms and molecules and the repulsive atomic forces that prevent material collapse. Failure of solids is possible only because the net attractive force between atoms is strongly and inversely dependent on interatomic distance. When the interatomic distance is increased sufficiently, as for example by application of external force, tensile failure occurs. All material failure is tensile at the atomic scale.

The behavior of bulk granular materials is strongly affected by the angularity of the grains. Smooth grains generate less resistive force (friction) under load than rougher grains. Quantification of grain angularity has been attempted using spectral analysis, fractal analysis, and comparison with standard profiles. The last, although somewhat subjective, is the most common approach. Statistical analysis of two-dimensional digital images is readily automated for this purpose.

Decades of comminution research (Prasher, 1987) have revealed the following relationships:

- More energy is required to crush a bed of small particles than one consisting of large particles. Some authors attribute this to the linear relationship between particle surface area and the energy required to produce the particle.
- Particle breakage results in a bimodal size distribution of descendent chips. The very small particles (fines) are created within a lobe of intense stress concentration immediately beneath the applied force. The coarser chips are from breakage of the rest of the particle.
- A monomodal particle size distribution emerges eventually with continued grinding beyond primary breakage.

- Whatever the size distribution of the initial material, a given material will produce a characteristic size distribution after continuous grinding.
- Viscoelastic materials such as permafrost are more sensitive to strain rate, that is, force application rate, than brittle materials are. Viscoelastic materials are better fractured at high strain rates, for example, by impact, than by slow compression (Brady and Brown, 1992).
- There is a "grind size limit" below which the material behaves plastically, regardless of its behavior at larger sizes.
- Material breakage is controlled by its fracture energy. Free surface energy is several orders of magnitude below fracture energy.
- Multiple fracture events produce more fines than single large fracture events, given that both expend the same amount of energy.
- The average energy efficiency of grinding processes ranges from 5 to 15%, with most less than 10%.
- As impact energy increases, the efficiency of the transfer of energy to particle breakage decreases.

For percussion drill systems, primary breakage occurs when the chips are first formed from the initially intact natural material, whether it is unconsolidated or consolidated. Stage I of comminution begins beneath the bit with the next blow of the percussion mechanism. The conditions there are most closely simulated by full-confinement bed tests. The utilization of the applied energy, expressed in terms of new surface area produced per unit of externally applied energy per unit mass, varies with the material being crushed. Dynamic testing of beds of cement clinker indicates that larger initial particle size also increases energy utilization. This supports the notion that larger particles are weaker than smaller particles, and by producing more new particles thus create more new surface area for a given energy expenditure.

Modern roller mill design is being supplemented with ultrasonic vibration to enhance the comminution process, generally at frequencies of 10–20 kHz (see, for example, Graff, 1979; Lo and Herbst, 1990; Lo and Kientzler, 1992). Useful frequencies reduce particle density within the bulk granular material in the immediate vicinity of the borehole. In some loosening regimes of vibrational frequency and amplitude, the material recompacts when the vibration ceases, potentially seizing the bit or mole and locking it in place (R. Gustafson, Orbital Technologies, Madison, WI, personal communication, 2008). Full experimental characterization of the frequency–amplitude–material properties space for natural or artificial sediments has not been completed, although efforts are under way (e.g., Kim and Drabkin, 1995; Rémond, 2003).

Several semiempirical "energy laws" have been developed for comminution, including those of Von Rittinger (applicable to cuttings of 10–1000 μm diameter), Kick (cuttings greater than 1 cm across), and Bond (intermediate sizes). The Bond work index is assumed to be a characteristic resistance of the material to crushing; in practice, it is expressed in terms of the energy per unit mass required to reduce the particle size from theoretically infinite diameter to 80% passing 100 mm. However, the breakage characteristics of rock are not constant over all sizes. Therefore, the Bond work index is measured industrially at specified standard grind sizes using a careful procedure. Ironically, the strict test procedures are so time consuming that several simpler methods have been developed to obtain indices to relate to the Bond work index (Wills, 1992).

3.4.4.2 Packing

Compaction of drill cuttings within unconsolidated sediments in the immediate vicinity of the drill bit is possible for a limited amount of cuttings. The amount is dependent on the porosity and size distribution of the original sediment and the size distribution of the cuttings. Compaction of granular material is essentially the same collection of phenomena as convection (see below), but without the particle circulation components. The initial porosity in sediments is controlled by particle size, particle shape, and the distribution of particle sizes. In material composed of a monomodal particle size distribution, the force needed to overcome frictional and cohesive bonding forces increases with the exposed surface area of the particles. Since particle specific surface area is inversely proportional to particle size, a unit mass of fine particles stabilizes at a larger porosity than a unit mass of coarse particles (all other factors being equal). There is a trend towards increasing porosity as particle size decreases, but it is significant only for diameters below 100 mm. As particle diameter increases, the effects of friction/cohesion decrease and a limiting value of initial porosity is reached.

3.4.5 Creation of Disposal Volume

Bulking of rock particles can be accommodated *in situ* by increasing the pore or fracture volume available for their disposal, in addition to reducing the volume they occupy (packing, above). In unconsolidated media, disposal volume can be increased by compacting the surrounding material radially and tangentially in the immediate vicinity of the borehole. In brittle elastic rock, this can be done by creating and opening fractures that intersect the borehole. In both cases, especially the latter, effective use of the disposal volume requires transport of the cuttings into it.

3.4.5.1 Compaction of *In Situ* Material

In unconsolidated media, devices such as cone penetrometers advance by compacting the medium around them. This works best in loosely packed sediments, which compress under load. It works less well in densely packed materials with wide size distribution curves that bulk in the same situation.

Compaction of unconsolidated material is accomplished by (Guéguen and Palciauskas, 1994)

- pressure (static input of energy)
- vibration (dynamic input of energy).

Compaction of unconsolidated material surrounding the borehole incorporates crushing and repacking of the grains. In solid rock, the relative contribution of the latter becomes negligible at less than extremely high pressures. The mechanical aspects of compaction consist of:

- rotation and sliding of grains
- pore collapse
- fracturing between grains
- fracturing within grains.

Irreversible compaction (i.e., material failure) occurs in hydrostatic conditions when the compaction pressure exceeds a critical pressure. The stiffness and strength of granular materials rise significantly when even a minor amount of cementation exists at the grain–grain contact points (Dvorkin, Mavko and Nur, 1991; Dvorkin, Yin and Nur, 1994; Zang and Wong, 1995; David, Menéndez and Bernabé, 1998). Any type of ice (water, carbon dioxide, etc.) deposited within the pores of sedimentary material serves as natural cement. As the volume fraction of cementation increases, the transition from brittle to ductile behavior occurs at higher stresses, the critical pressure increases, the bulk modulus of the rock increases, and the material compressive strength increases beyond that of either the original material or the pure cement, but only up to saturation (complete filling of the original pore volume with the cement). At ice concentrations above saturation, increasing ice content decreases the bulk strength to below that of the pure ice until the amount of dirt in the ice becomes negligible (Tsytovich, 1975; Jeremic, 1987).

3.4.5.2 Fracturing of *In Situ* Material

As described by Bažant (1985) and Atkinson (1987), the fundamental modes of rock fracture have been categorized as follows:

- Mode I pure tension, where the walls of the fracture are pulled apart
- Mode II in-plane shear, where the fracture walls slide on each other
- Mode III lateral shear, or tearing mode.

The theoretical mechanics of fractures created by pressurizing boreholes are based on the assumption that only Mode I fracture occurs. In reality, rock and soil satisfy these criteria only partially, and even so, the fracturing changes to mixed mode once the crack begins to propagate. Therefore, a more rigorous theory of fracture mechanics has been developed, which is still in the early stages of being applied to drilling.

Static loading of rock is a special case of general dynamic loading, where the loading period is infinity. At long load periods, the rock failure response is independent of time, and linear relationships between strain or stress and strength are adequate. However, dynamic yielding of statically overstressed rock depends on loading rate, load intensity, and load duration; in other words, dynamic rock failure depends on a minimum dynamic fracture energy.

3.5 Directional Drilling

One of the issues in ground drilling is borehole trajectory control. If a drill deviates from a direct path to a target, additional penetration, with the accompanying energy expenditure and bit wear, will be required. How does a drill handle odd-angle interfaces such as might be encountered with a boulder buried in the regolith? Or what if a drill should encounter a hard streak from a basaltic flow of lava? In this section, the issues related to directional drilling, as these issues are called in the petroleum industry, will be discussed.

It has been said that the only straight and vertical borehole is in a textbook. Every borehole deviates from the direct path to a given subsurface location (often called a target). This was recognized early in the evolution of drilling. As John Hoffman said in 1912, "Every borehole dips from the vertical." In 1920, Hall and Row said, "All holes tend to curve and take somewhat erratic courses." This tendency of boreholes to deviate fuels a multi-billion dollar petroleum and mining service company industry.

3.5.1 Reference Systems

The most important item concerning directional drilling is maintaining one's orientation in three-dimensional space (Figure 3.12). The target is the location in

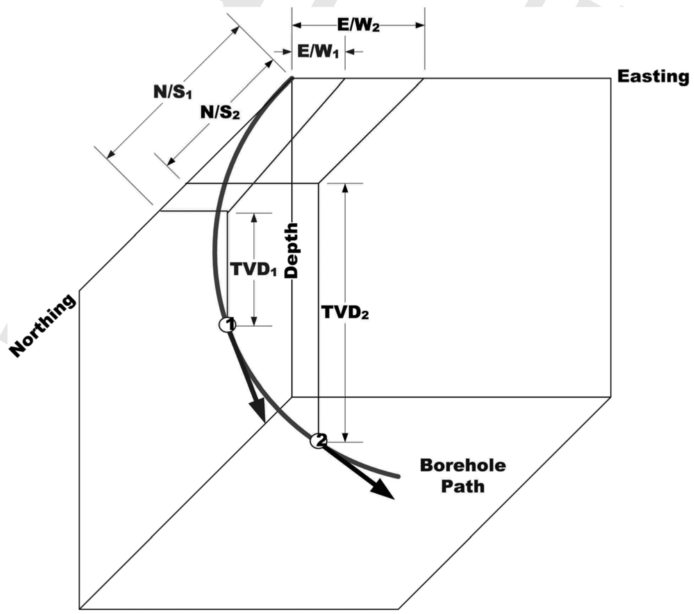

Figure 3.12 Borehole path and stations.

three-dimensional space. It is the spot (or spots) that one aims for in directional drilling. This spot is usually designated by a north/south (N/S), east/west (E/W), and true vertical depth (TVD) coordinate or by an azimuth and a TVD. Although it is usually described as a specific location, it is actually the volume surrounding the target that one is interested in entering. As such, the greater the volume, the less challenging the requirements are for entering the target volume. To put it another way, the wider the target, the easier it is to hit.

All boreholes are referenced to the surface location. A station is a measured point in underground three-dimensional space. There are three measurements needed at a station for orientation: inclination, azimuth, and measured depth.

Inclination (ϕ) is referenced to the angle relative to a vertical line at a survey station. Inclination is 0° for a vertical borehole and 90° for a horizontal borehole. Should the borehole cross through 90° and start towards the surface, the borehole inclination is stated to be greater than 90°.

Azimuth (θ) is the angle referenced from true north to the horizontal direction of the borehole. It is measured from 0° being true north clockwise (looking down on the surface location) to, but not including, 360°.

The measured depth (MD) is the distance along the borehole. This depth is positive and is referenced to the surface location. All other directional drilling values can be derived from these three data. One very important derived data is TVD, which is the vertical depth to the station; it is the "how deep are you relative to the surface of the planet (moon, asteroid, etc.)?" Other important derived data include the departure and section. Departure is the direct horizontal distance to the measurement station. The section is the projection of the departure to the vertical plane that bisects the surface location and the target.

This data can be further derived to determine the three-dimensional point in space that a survey station represents. The typical method is to convert the previous data into Cartesian coordinates. These are referenced to the surface location of the borehole and to true, magnetic, or grid north. The coordinates are listed in terms of distance from the reference in terms of the north or south and of east and west of the borehole. The convention is for north and east coordinates to be positive. In addition, depth coordinates are always positive.

The borehole has a defined geometry (Figure 3.13). For example, the borehole will have a top side and bottom side relative to gravity (except for the unusual case of a perfectly vertical borehole). The top of such a borehole is called the highside of the borehole and is defined as 0° relative to the borehole. Conversely, the bottom of the borehole is called the lowside and is defined as 180°. A right turn would be to the 90° area of the borehole and a left turn would be towards the 270° area of the borehole (visualized as the bit "sees" the bottom of the borehole). The toolface angle is defined as the direction of the bit relative to the borehole. For example, if the orientation of the bit was high and right relative to the borehole, then the toolface angle would be between 0° and 90°. Drilling with the bit in that direction would, in all likelihood, cause the borehole to increase in angle and turn towards the right.

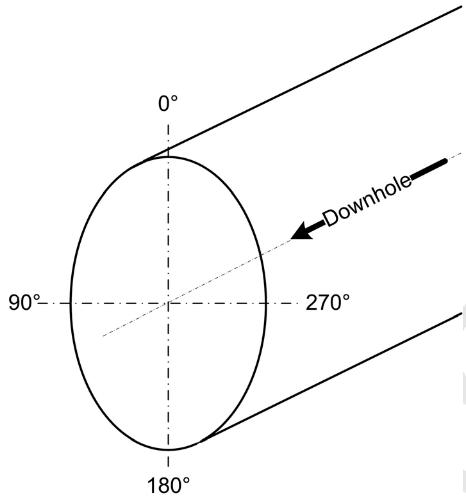

Figure 3.13 Toolface orientation.

3.5.2 Directional Control Factors

There are many factors that affect directional control, including geology, borehole conditions, bit design, and bottom hole assembly design.

3.5.2.1 Geology

The subsurface geology of any extraterrestrial body is a large, unknown factor. If surface photographs are an indication of subsurface conditions, drilling will be difficult. On Mars, for example, formations with boulders and cobbles of differing rock properties than the surrounding material are some of the most difficult geological materials to drill. One penetration shape may work well with one type of rock but will fail utterly with another. The cuttings transport may work well with the cuttings from one type of rock and flounder with another.

3.5.2.2 Macro-Geology

The overall *in situ* structure of a rock will affect drilling. There are three *in situ* structures of importance to drilling: the inclination and direction of a layer of rock, the degree of fracturing, and the overall geological structure. The following discusses some of the effects of this macro-geology.

The inclination and direction, called dip and strike, respectively, by geologists, of a layer of rock (bedding plane) strongly affect the directional control of a drilling system. The dip of a formation is a measure of the inclination of a formation layer. The dip angle is 0° for a horizontal layer, just the opposite of the borehole inclination reference. The strike is the horizontal orientation of a formation layer (Tarbuck and Lutgens, 1999).

The effective dip angle is the angle at which the bit intersects the rock layers. For vertical boreholes, the geological dip angle is the effective dip angle. If the borehole inclination is 25° and the geological dip angle is 30°, and the strike in the borehole direction, the effective dip angle is 5°. For example, if the borehole inclination is 25° and the geological dip angle is 30°, but in the opposite direction, the effective dip angle is 55°, and the borehole will deviate downwards. If the directions of the borehole and strike are not collinear, then right and left borehole trajectories will result. The directional control of a drill system also depends on many other factors, such as bit force direction and tilt angle, which will be discussed later.

There is a rule of thumb in drilling concerning dip angles. If the effective dip is 45° or less, the borehole will tend to drill perpendicular to the dip (cross dip). If the effective dip is 45° or more, the borehole will tend to drill parallel to the dip (down dip). Typically, formations are harder the deeper one drills. When a dip is shallow, as the borehole crosses from the softer higher layer to the harder lower layer, the bit will drill the harder side more slowly than the softer side. This results in a bending moment towards the harder layer. Hence the bit drills perpendicular to the dip. When the layers are steep, the bit will tend to deflect off of the harder layer, resulting in a bending moment parallel to the dip. Of course, should the formations have varying hardness, the bit will tend to wander.

The amount of fracturing within a rock bed will have an effect on drilling. The fracturing can be in all sizes and directions. A fault is a macroscale fracture and cleating (small fractures within a rock structure) is a microscale fracture. An example of the former is the San Andreas Fault in California and an example of the latter is coal. The degree of fracturing will be a factor in the ease of rock failure. The more fracturing, the greater is the ease of removal. However, under those same conditions, the cutting structure may not load evenly and fail, because of bit bounce from the sudden failure of a fracture plane.

Geological structures will have an effect. For example, an anticline (warping upwards of the geological structure) will tend to cause a borehole to deviate into the interior of the structure. Conversely, a syncline (warping downwards of the geological structure) will deviate the borehole away from the structure. A borehole trajectory may be erratic depending on the size and nature of a fault (a fracture in the geological structure). A fault may also cause drillability problems as a bit crosses the fault zone. Finally, an unconformity (a break in the depositional record) can cause radical changes in borehole trajectories.

3.5.2.3 **Rock Properties**

The rock property characteristics will also affect borehole trajectories and drillability. Q2 Rock properties are discussed more thoroughly in the Rock Properties chapter. However, rock properties will affect directional drilling. These rock properties include the strength, hardness, stress/strain behavior, and abrasiveness (Jimeno, Jimeno and Francisco, 1995).

Rocks consist of a crystalline mineral or mixture of minerals. These minerals are subject to weathering, deposition, compaction, and heating and cooling. It is this lithological history of the mineral or mineral mixture that will have a major effect on its material structure and properties.

As liquid minerals cool, crystals will form. Depending on the cooling rate and mineral chemistry, the crystals will be of various sizes, from less than 0.1 mm to large structures. These crystals, called grains, will be cemented together by some other mineral along the grain boundaries. The degree of interlocking, the strength of the cement, and the grain size and material, along with its aforementioned lithological history, will dictate the rock properties.

The strength of a rock is its ability to resist tension and compressive failure. A rock is usually stronger under compressive stresses than in tension stresses. A rule of thumb is that the tensile strength of a rock is about 10–15% of its compressive strength. This is because the compression stress is loaded through the grain structure whereas the tensile strength depends on the adhesion between the grains. Unfortunately, the only way to load a rock in tension *in situ* is to overcome its compressive strength in order to split the rock.

The grain shapes and sizes will also have an effect on the strength. Rounded shaped grains tend to be easier to drill than other shapes. Generally, the smaller grain sized rocks tend to be stronger. In addition, the stronger cementation material makes for a stronger rock. Finally, low-porosity rocks tend to be stronger. The fluid content of the rock will also have an influence.

The strength of a rock will tend to be anisotropic. Some rocks will be isotropic and homogeneous, but these are rare. Most rocks have some degree of anisotropy and inhomogeneities. For example, a mica is relatively strong perpendicular to its layered structure but fairly easy to part parallel to its layered structure. This effect is discussed in more detail later.

A soft rock is defined as one with a compressive strength of less than 5000 psi. A hard rock is defined as one with a compressive strength greater than 15 000 psi. All other rocks are considered medium strength rocks.

The hardness of a rock is the resistance of the rock to penetration. This property will tend to drive the selection of the drilling method, because the rock must first be penetrated before it can fail and be removed. The rock hardness is related to its composition. The mineral make-up of the rock generates its hardness. For example, a rock consisting of quartzite will be harder than one consisting of limestone. As before, the porosity and fluid content will have an effect on the hardness of the rock.

Rocks will exhibit an elastic or plastic behavior. Most rocks exhibit brittle elastic failure. That is, the rock will elastically load under Hooke's law behavior until the rock yields and fails immediately thereafter. However, there are other types of rocks that will deform plastically prior to brittle failure or will simply deform plastically. An example of the former rock would be shale under high pressure and the latter unconsolidated sand.

The degree of elastic/plastic behavior depends on many factors. This material property can be characterized by its modulus of elasticity, E, and Poisson's ratio, ν. The material construction of the rock and the manner of cementation will have a major effect on this behavior. The harder the grains and cement, the higher the modulus of elasticity will be. Also, the temperature and pressure of a rock will also affect E. Rocks that are at 300 °C will show a marked difference in material properties. These hot rocks will exhibit a far more plastic behavior than at room temperature and pressure.

The abrasiveness of a rock has profound consequences for the life of a cutting structure of a drill. The higher the abrasiveness of a rock, the shorter the lifetime a cutting structure will have. Even tungsten carbide will wear away in the span of a few meters in some rocks.

The quartz content is the usual indicator of abrasiveness. Quartz grains are some of the hardest grains in a given rock. In addition, the shape and size of the grains will affect abrasiveness. Grains that are angular will exhibit higher abrasiveness than rounded grains. Larger grains will also exhibit a higher abrasiveness than a smaller grain structure. Finally, heterogeneity of the rock, including its porosity, will give rise to localized surfaces that will be more abrasive.

3.5.2.4 Borehole Conditions

The borehole conditions will affect the directional trajectory characteristics. These conditions include gauge, stability, and trajectory.

If the borehole distorts to a size greater than the bit diameter, the borehole is said to be overgauge; if the borehole is the same size as the bit, it is in gauge; and if the borehole is smaller than the bit size, it is undergauge. The directional characteristics of a drilling system depend on a good fit within the borehole. An overgauge borehole will allow a loose fit for the drilling system. That means that the directional control qualities of the drilling system will suffer with unpredictable results.

The borehole stability will have an effect. If the borehole collapses, a drilling system will not have any room to maneuver. The sidewall friction will also be larger, changing the forces upon the drilling system. If the borehole is soft, directional control could be lost. Since the directional control equipment of a drilling system depends on a solid base from which to exert forces, a soft borehole will allow a drilling system to “mush” and not deviate predictably.

The previous borehole trajectory will have an effect. A curved borehole will cause the trajectory control forces of a drilling system to point in a different inclination and direction than the trajectory control forces in a straight borehole. In addition, if the azimuth of the borehole is in a different direction than desired, the larger the azimuth change, the further it will take to effect the change.

3.5.3 Bit Design

The bit design is critical to the directional characteristics of a drilling system. There are two factors that control borehole trajectory: bit tilt and side force. These two factors are affected by the bit type and thrust, ROP, stabilizer placement and fit, bottom hole assembly stiffness and length, and formation characteristics. The interaction of these two effects dictates the direction of the bit force, which in turn dictates the borehole trajectory.

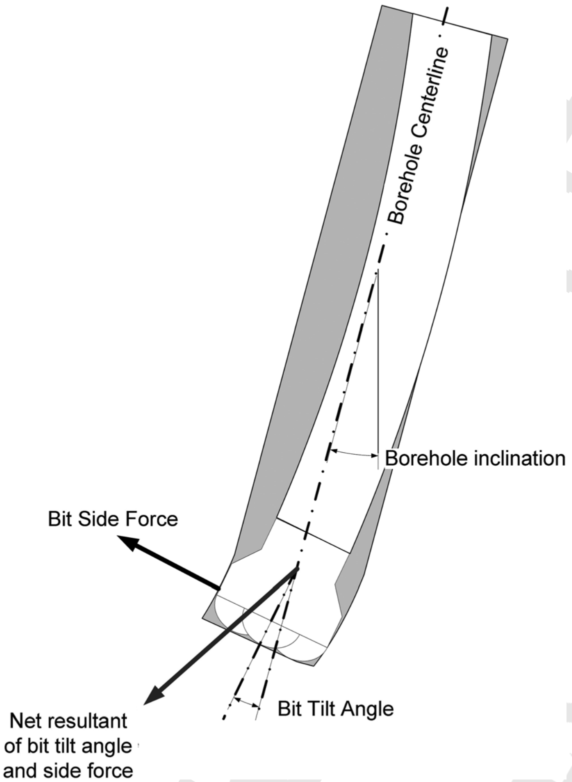

Figure 3.14 Directional drilling forces and angles.

There are two methods for directionally controlling the trajectory of a bore hole: either to push the bit in the desired direction or to point the bit towards the desired direction (Figure 3.14). Pushing the bit involves using basic leverage through the correct placement of stabilizers (to act as a fulcrum) and the drill string equipment [known as the bottom hole assembly (BHA)] and a bit that can cut along its side. Pointing the bit typically involves a physical mechanism that aligns the rotational axis of the bit so that it is non-coincident with the rotational axis of the BHA. This mechanism can be a connector (called a "sub") that has the threads on either end cut non-axially with the body of the sub or a bend in the bottom hole assembly motor. The BHA motor (often called a mud-motor and based on a Moineau-style pump) is a positive displacement fluid-driven motor on the bottom of the drill string. To use either method indicated above, the drill string cannot be rotated while directionally drilling (called slide or oriented drilling). To go straight, the string can be rotated, thus not aligning the bit in any preferred direction.

While in oriented mode, the static friction from sliding limits the distance that a hole can be drilled. With today's distance out from under a well site reaching 10 km, friction is a serious problem. To overcome static friction, the drill string can be rotated, allowing dynamic friction to predominate, which is a smaller value than under static conditions.

To do that and drill directionally requires a totally different directional drilling system, called a rotary steerable system. These come in two styles, push the bit and point the bit (which is the same as noted earlier).

The first to come out in the mid-1990s was the push the bit system, now called "Powerdrive" by Schlumberger. The bottom motor has a set of push levers to pop in and out constantly depending on the orientation of the assembly. For example, if the assembly was to build angle, the lever would be at full extension while rotating past the bottom of the hole and in full retraction 180° later and return to full extension another 180° later back at the bottom of the hole. With three levers, the assembly has a continuous push in the desired direction.

In contrast, a point the bit system has the bit on a bent assembly that is attached to the main motor. This assembly is attached by a system that rotates the assembly in the exact reverse of the rotation of the drill string. This keeps the bit pointed in the same direction at all times. The bit still rotates from the mud motor spin.

Dareing first proposed the bit tilt effect in 1971. The term "tilt angle" was assigned to this work. Tilt angle is the angle between a line perpendicular to the base of the bit and the centerline of the borehole (Figure 3.14). This is the application angle of the bit force. The bit force is the load on the bit that generates the rock failure at the face of the bit. It is often called thrust in mining terms or weight-on-bit in petroleum terms.

The bit tilt depends on the shape of the cutting structure, the overall shape of the bit, and the assembly above the bit (to be discussed in Section 3.5.4). A short cutting structure will allow a larger bit tilt angle than a longer cutting structure, assuming that the cutting structure is engaged in drilling. An analogy is a short versus long shovel. A short shovel is easier to manipulate than a long shovel. However, a short shovel will not dig as fast as a long shovel.

Similarly, a flat, short, even concave, overall bit shape will be easier to tilt than a long tapered overall shape. This is called a crown profile. A flat, short crown profile will have a smaller contact area along its sides, allowing for pivoting to occur. A long tapered crown profile will have a larger side contact area, providing more stabilization.

The side cutting ability of a bit is related to the side force. If a bit is pushed into the side of the borehole, depending on the crown profile and cutting structure, the bit will drill in the direction of the side force. This side force can be up or down, right or left.

The degree of bit tilt and side force dictates the magnitude of directional control. This bit tilt will have a major effect in hard formations whereas the side force will have a major effect in soft formations. If there is an uphole side force and uphole bit tilt, the borehole trajectory will tend to build angle. Conversely, if there is a downhole side force and downhole bit tilt, the borehole trajectory will tend to drop angle. If there is an uphole side force and downhole bit tilt, the borehole will tend to drop angle in hard formations and build angle in soft formations. If there is a downhole side force and uphole bit tilt, the borehole will tend to build angle in hard formations and drop angle in soft formations.

3.5.4
Bottom Hole Assemblies

The bending of pipe above the bit influences borehole deviation tendencies (Hoffmann, 1912). A BHA is defined as the part of a drillstring that controls the direction and penetration. For typical drilling rig operations, the BHA consists of large, heavy pipe sections (joints) called drill collars. These allow the application of force on the bit without severe bending. There are also many other pieces of equipment for specialized applications. These can be logging (LWD) and drilling (MWD) parameter measurement instrument packages. There can be motor packages and shock absorbing and application (jars) tools. In addition, there can be stabilizers.

Stabilizers are placed in a BHA to control the direction of the entire drillstring. The placement of stabilizers is based on fulcrums. A short stabilizer will tend to act as a pivot whereas a long stabilizer will tend to center an assembly. By judicious placement of the stabilizers, proper material and geometric properties of a drillstring, and sound operational parameters, the driller can control the directional tendencies of a drilling assembly.

For example, by placing a short stabilizer near the bit as shown in Figure 3.15a, a BHA can be made to pivot about that point. This, in turn, tilts and applies a side force at the bit. Depending on the stiffness and orientation of the assembly above the stabilizer, the bit can be made to drill directionally in the desired direction. Since most strings tend to lie on the low side of the borehole, the bit tilt and side forces will tend towards the high side of the borehole. This type of assembly is typically used to build (increase) the inclination angle of a borehole.

On the other hand, if this same short stabilizer is placed further away from the bit as shown in Figure 3.15b, the BHA will again pivot about that point. However, since the pivot point is further up the borehole, the tilt and side forces will tend towards the low side of the borehole. This type of assembly, called a pendulum assembly, will tend to drop (decrease) the inclination angle of the borehole.

Should two or more stabilizers, one near the bit and one further away from the bit, be used, as shown in Figure 3.15c and d, the assembly would not tend to pivot but rather be stiffer.

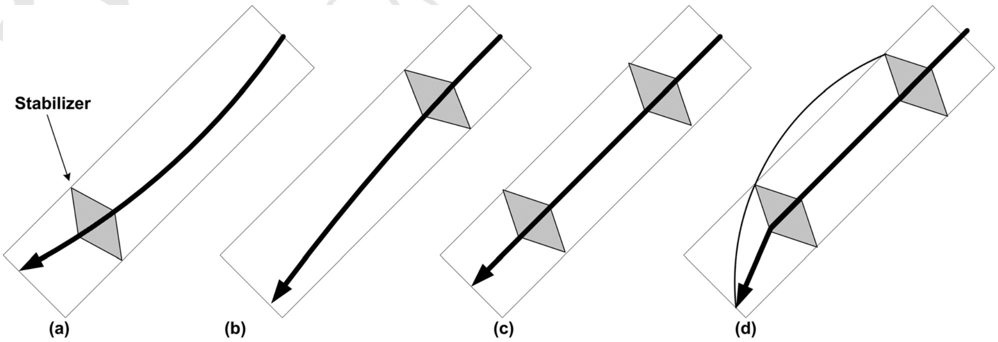

Figure 3.15 Stabilizer placement effects.

If the bit and these two stabilizers are collinear, this will tend to keep the borehole straight. This kind of assembly is called a packed hole assembly (Figure 3.15c). If the bit and the two stabilizers are not collinear, the assembly will describe an arc. This is called three-point geometry and is the basis of direction control in the petroleum industry (Figure 3.15d). The assembly will drill an arc. The radius of the arc depends on the distances from the bit and stabilizers and the degree of the angle that the bit and stabilizers form and also the geology and drilling operations parameters (Cerkovnik, 1998; Williams, 1998; Schlecht, 1999).

The stabilization assumes that the stabilizers are in contact with the borehole walls. Often, the size of the borehole is greater than the diameter of the bit that drilled it. This condition can cause great difficulty in maintaining trajectory control. Unless the stabilizers can be downhole adjustable, the contacts needed for pivoting or stiffening will not be available or, worse, will be far enough away to cause the bit tilt and/or side forces not to be predictable. Often this condition explains why bottom hole assemblies sometimes behave unpredictably.

3.5.5
Directional Mechanics

Although directional drilling was being accomplished from the early 1900s, it was not put on a rigorous mathematical footing prior to Arthur Lubinski's pioneering 1950s papers. His first paper in 1950 explained the buckling tendencies of a BHA and how this could lead to deviated boreholes. His 1951 paper with MacDonald pointed out how stabilizers in strategic locations along a BHA could straighten an otherwise deviated borehole (Figure 3.15). His 1953 paper with Woods introduced the formation anisotropy index and equilibrium angle concept.

Lubinsky and Woods invented the concept of anisotropy in 1953 to explain why a bit drilled in a different direction than the bit force direction. The drilling anisotropy index is defined as the relative difference in rock drillability parallel and perpendicular to the dip. An index of zero meant that the formation was isotropic. If the index was not zero, even if the bit was drilling perfectly perpendicular to the dip, the bit would still deviate.

The anisotropy index, although not totally understood, is thought to be the result of a rock failing unevenly. An anisotropic rock will tend to fail more in one direction of the borehole than in another. This causes the chips generated on that side of the borehole to be larger on the more easily failed side. This causes uneven chip volumes around the bit and a subsequent force generated on the side of the bit. This force is added to the bit side force generated by the entire drilling assembly. This then drives the borehole trajectory.

The equilibrium angle is the inclination and azimuth which a borehole will tend to follow given no change in thrust, borehole size, formation characteristics, gauge, and so on. This means that a bit will eventually settle on a stable borehole trajectory. However, if any of the aforementioned factors change, the borehole will once again seek its equilibrium angle.

3.5.6 BHA Modeling

BHA modeling is extremely important for trajectory control. The modeling of the directional response input with the resulting output will be critical to the success of directionally controlling any drilling system. In addition, by knowing the directional response characteristics of a drilling system, it might be possible to infer the geological characteristics of the medium being drilled.

Since drilling in extreme environments will likely be remote, an active autonomous control system will be required. There are no rules of thumb or prior knowledge of drilling conditions in extreme environments. Local geology and directional tendencies will be unknown. An active control system must be built into a drilling system. A drilling system must be capable of adapting to local conditions and still carry out the mission.

BHA models today fall into two categories: equilibrium models and drill-ahead models. All models generally attempt to determine side forces at the bit and stabilizers. This gives the directional tendencies of a particular BHA and bit combination. The models do not attempt to determine the actual bit displacements in three-dimensional space.

3.5.6.1 Equilibrium Model

The equilibrium model is based on a static equilibrium 2D inclined beam. The beam shape and reactions are determined and a borehole curvature is predicted. All of the known controllable static forces (thrust, weight, etc.) are applied to the model. Derived loads (bit side forces from formation anisotropy, etc.) are also applied. However, since the bit and formation anisotropic effects are inferred, this model can be less accurate than the drill-ahead model. In addition, another limitation to the model is that dynamic effects are not considered. The advantage is that the model less computationally intense than the drill-ahead model.

3.5.6.2 The Drill-Ahead Model

The drill-ahead model is based on a force vector approach. The three-dimensional static and dynamic force and torque vectors are applied to determine a borehole path. The effects of geology (dip, strike, anisotropic effects, etc.) are included. The borehole trajectory increments generated in this method are on the order of centimeters. Therefore, this type of model can be computationally intensive.

3.5.6.3 General Bottom Hole Assembly Modeling

The first to define mathematically a BHA with two stabilizers was Hoch (1962). He suggested using a near-bit stabilizer to limit lateral bit movement.

Bogy and Pasley (1964a) analyzed the buckling tendencies of an unconstrained drillstring on an inclined plane. A second paper by Bogy and Pasley (1964b) continued the previous work by constraining the drillstring to a rigid, cylindrical inclined borehole. This was accomplished by analyzing the stability based on minimum total mechanical potential energy. Walker (1973) continued the previous work by adding the ability to model buckling with multiple stabilizers.

Q4 Fischer presented a finite difference model of the static deformation of a BHA within a curved borehole in 1974. The BHA consisted of a finite number of constant-property beam columns. The borehole consisted of vertical circular arcs and line segments with varying borehole diameters. An iterative procedure for wall contact boundary conditions was required in the analysis.

Q5 In 1977, Walker and Friedman developed an analytical differential equation model. This model was based on a static, three-dimensional, inclined borehole BHA. This model investigated the building, dropping, and turning tendencies of BHAs via the bit force angle results. For the first time, torque was considered. It appears from this model that torque is not a large factor in directional control.

A finite element method (FEM) for BHA modeling was developed by Millheim, Jordan, and Ritter in 1976 (presented in 1978: Millheim, Jordan and Ritter, 1978). Various BHAs were modeled to attain the side force at the bit. It was a static, two-dimensional model with straight, inclined borehole geometry. This may explain why the results were inconclusive as compared to field BHA responses.

Further work by Millheim (1977) incorporated into the previous FEM model three dimensions and a curved borehole. Field data analysis, experimental test drilling, and the computer model showed that borehole curvature and its effects are one of the most important variables in predicting and controlling borehole trajectory. Millheim presented the following observations:

- All well paths exhibit an oscillatory behavior. This behavior is dependent on the bit thrust load, design, borehole size, formation type, and BHA configuration.
- Borehole curvature effects the prediction of the borehole trajectory and the application of bit thrust load.
- Initiating a build angle in soft to medium soft formations is more difficult than in harder formations. Once started, the borehole will build angle at either steady state or accelerate.
- A change in BHA configuration may result in a transient “follow through” of the previous BHA directional tendency. This is attributable to borehole curvature.

Millheim made further observations in an eight-part series of articles in the *Oil and Gas Journal* (Millheim, 1978a–d, 1979a–d):

- The adjustment of bit thrust load provides some leverage for partial control of the bit side force. However, the higher the borehole inclination, the less is the effect.
- An angle holding BHA is sensitive to borehole inclination. This is because the side forces exerted by the bit and BHA vary depending on the formation being drilled. The “rules of thumb” for holding an angle are:
- Make as few changes to drilling operating parameters as possible.
- Use the simplest BHA.
- Make the angle holding section short.
- Very soft formations have the following effects:
- Dip and strike have little effect on borehole trajectory.

- It is easy to change trajectory with a flexible BHA.
- It is difficult, maybe impossible, to change trajectory with a stiff BHA.
- The structural effects of dip and strike are the most pronounced in medium soft and medium strength formations.
- Lithology change is not as important to trajectory control as is hardness variations.
- Penetration rate will affect the ability of a given BHAs directional tendencies.
- The harder the formation, the slower the response of an angle dropping BHA. However, the higher the inclination, the faster the response.

Millheim and Apostal (1981) stated that the dynamic effects of geology, borehole condition, bit rotation and the friction of the stabilizers, pipe, and bit must be considered in predicting the BHA borehole trajectory response. By adjusting the borehole diameters and by tuning the friction factors for the bit, stabilizers, and pipe, their history matched five shallow, experimental directionally drilled wells.

Using an FEM, Toutain (1981) showed that for azimuth control, the most critical parameters are bit–wall contact area, bit or stabilizer borehole wall clearance, and borehole curvature. They also reiterated the oscillatory nature of borehole trajectory and it appears smooth only in the average sense.

Q6 In 1981, Callas presented an analytical approach with a two-dimensional bending model. The author called this a drill-ahead model. The borehole trajectory is computed iteratively and is based on the equilibrium angle, the force angle between the bit thrust and side force angles, the borehole curvature, and various "other heuristic factors." Enen, Callas and Sullivan (1984) improved the model by the addition of an empirical parameter which rated how much a particular bit drills to the side as opposed to drilling along its axis. The empirical factor is used to tune the program to history match a previous bit effects.

Brett *et al.* (1986) developed a three-dimensional, static finite element model. The drill-ahead model based on this work is

$$\phi^{n+1} = \phi^n + \beta_x + \arctan\left(\frac{P_x}{P_z}\right) \tag{3.37}$$

where

$$P_x = \frac{A}{r} S_f^2 \tag{3.38}$$

and ϕ^{n+1} is the next bottom hole inclination, ϕ^n is the current bottom hole inclination, β_x is the bit tilt angle, P_x is the bit lateral penetration rate, P_z is the bit axial penetration rate, the A is an empirical constant that models directional response of BHAs, S_f is the total bit side force, and r is the dimensionless rock strength.

Note that the bit type and size are neglected and also no dependency on time or space. In addition, it is very difficult to determine many of these factors such as the various penetration rates. However, the model does exhibit many of the tendencies of field examples such as oscillatory behavior.

Ho (1986) determined a generalization of existing drill-ahead models with a drilling vector. This vector was modeled as a linear function of the resultant bit force, statically deflected bit axis, and the normal to the formation bedding planes. Another drill-ahead model by Rafie (1988) predicted a transient inclination angle. The model was based on inclination angles, measured depth, and the resultant force angles between the current and previous survey stations. Additional papers on this subject were published by Baird *et al*. (1984), Rafie, Ho and Chandra (1986), Jogi, Burgess and Bowling (1986), Birades and Fenoul (1986), Williamson and Lubinski (1986), Brakel and Azar (1989), Spanos and Payne (1992), Heisig *et al*. (1996), and Neubert and Heisig (1997).

Adding rock–bit interaction to BHA models complicates the problem. The eccentricity of the axial force (relative to the bit axis) to the bottom of the borehole, the lateral forces between the bit and the bottom and walls of the borehole, and the side cutting ability of the bit all affect borehole trajectories and are interrelated (Ma and Azar, 1986). Additional papers on rock–bit interactions include Murphey and Cheatham (1965), McLamore (1971), Enen, Callas and Sullivan (1984), Ho (1986), Eustes, Mitchell and Stoner (1994), and Eustes, Mitchell and Long (1995).

In Williamson and Lubinski's 1987 paper, they present the following statement: "The main limitation of using any computer model of BHAs is the reliability of input data. In particular, three parameters – hole curvature, dip angle, and stabilizer clearance – are difficult to obtain accurately and have as strong effect on the results" (Williamson and Lubinski, 1986).

3.5.7 Planning

The directional plan is critical to the success of any directional drilling operation. The plan must be designed to fit within the constraints of the target, the geology, and the drilling tool capability. For drilling in extreme environments, since one goal is depth, then the plan should be straight down from the drilling site. This is easier said than done. No borehole is straight and vertical. There will always be some inclination and azimuth associated with a borehole. There is also the opposite goal of subsurface maneuvering. If a drill should need the capability to maneuver, for example to avoid a large boulder, then an entirely different design than a straight hole type of tool will be required. A straight hole drilling system would imply a geometrically stiff body with a large taper penetration unit and a long body. A maneuvering drilling system would imply a limber, possibly articulated, body with a flat crown penetration unit and a short body. Of course, a drilling system can be designed with a little of both types for limited maneuverability with straight hole capability.

The maneuvering drilling system can avoid downhole problems by going around them, if possible, or reorienting itself for optimum penetration if it cannot. Going around or orienting the drilling system can optimize the penetration section of the drill for a given type of rock. This assumes that some kind of drill-ahead sensor is employed or, at a minimum, some kind of seismic program to image the subsurface.

In addition, should the drilling system deviate from the planned path, a maneuverable drilling system can be retargeted to return back on track. However, the maneuvering drilling system will be more complicated and, hence, prone to failure. Also, energy would be diverted to the maneuvering unit, leaving less energy for penetration and cuttings transport.

A straight hole drilling system has the advantage of simplicity. There is no need for moving equipment to direct the planned path of this drilling system. In addition, all energy would be directed towards penetration and cuttings transport. It has the disadvantage of having to penetrate everything it encounters. Also, should the straight hole drilling system deviate from the planned path, it would be exceptionally difficult to reorient the drilling system back to the planned path.

3.5.8 Survey Techniques

An accurate borehole trajectory description requires frequent survey data (White, 1912). At a minimum, a drilling system must be capable of surveying and relaying inclination, azimuth, and measured depth. There are a variety of survey techniques available. Typical directional surveying instruments used in the petroleum industry are either magnetic and/or gyroscopic based.

For inclination, there are two general methods: the pendulum or an accelerometer. The pendulum has limitations on accuracy and resolution and cannot be used in a moving environment. The accelerometer is more accurate and can determine borehole inclination and toolface orientation.

For azimuth, there are three general methods, two being the compass and the magnetometer. The compass is subject to unwanted external influences and has limited accuracy and resolution, whereas the magnetometer is more accurate and can determine its orientation with respect to an external magnetic field. The gyroscope is another method of azimuth orientation. A standard gyroscope depends on accurate initial alignment and is subject to precession. There are also issues regarding reliability and temperature sensitivity. Other tools on the market include the North Seeking Rate Gyro. This gyro orients itself within a gravity field. This gyro can determine inclination and azimuth. It is not subject to precession and drift. It is limited to low-angle and low-latitude boreholes.

Sometimes real-time information is needed. This is accomplish by bottom hole assembly tools known as MWD tools. The MWD measures (among many other items) the inclination and azimuth of the borehole. Some can also measure forces, torque, vibrations, pressure, rotational speed, and temperatures. These tools send information back to the surface for interpretation via pressure pulses in the drilling fluid or through long-wavelength radio waves. The baud rate for both methods is fairly slow, on the order of 12 bits per second.

Another tool is the LWD tool. In contrast to MWD, LWD measures rock properties (although there is some carelessness in the use of this terminology in the industry; see Schlumberger's oilfield glossary at http://www.glossary.oilfield.slb.com). Properties measured are typically gamma ray count, spontaneous potential, resistivity, density, and porosity. Recent tools add acoustic, nuclear magnetic resonance, seismic, and direct formation pressure measurements. Some of the data are sent up to the surface in the same manner as the MWD tool. Some of the data are stored in the tool for retrieval at the surface upon coming out of the hole.

For measured depth, the length of the drillstring or tether will need to be measured. Stretch and kinks may be a problem.

It is important to note that there are many inaccuracies inherent in survey techniques. These errors can be listed in two categories, systematic and random. Systematic errors are repeatable errors. These include calibration errors, mis-referencing, misalignment in the borehole, survey instrument accuracy, and survey technique inaccuracies. Also, depending on the azimuth survey technique chosen, other systematic errors include gyro precession errors and magnetic variations from natural and human sources. Random errors include malfunctions, recording and telemetry errors, tool flexing, and magnetic field fluctuations. Some of these errors can be both systematic and random, but not at the same time.

These errors will affect the location of a given survey station. The inclination, azimuth, and measured depth will have varying degrees of uncertainty. This will cause an "ellipsoid of uncertainty" around every survey station (Figure 3.16). This ellipse will grow with every additional survey station. This could be thought of as an expanding cone centered on the most likely location of the borehole. More information on this subject can be found in Walstrom (1969), Wolf and deWardt (1981) and Williamson (1999).

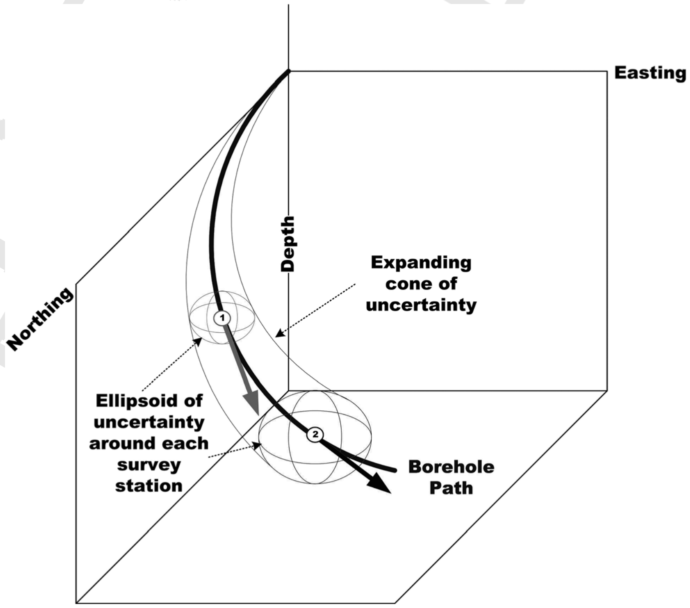

Figure 3.16 Ellipse of uncertainty.

3.5.9
Survey Calculations

Once the measured depth, inclination, and angle at a station have been determined, then various calculation algorithms are employed to locate the station position in three-dimensional space. These calculation algorithms, currently recognized by the American Petroleum Institute (API), include the backwards, forwards, and average tangential, radius of curvature, and minimum curvature methods. Each method will give the N/S, E/W, and TVD coordinates for a survey station. However, accuracy is not the same. It is accepted that the minimum curvature, based on an oblique circular arc, is the most accurate (Mitchell, 1995). Another oblique circular arc solution, known as the sectional method (Long and Mitchell, 1992), provides a simplified set of equations as shown below. This method was one of the first algorithms for accurate interpolation between survey stations.

The sectional method equations are as follows:

$$\Delta \mathrm{N/S} = \frac{\Delta \mathrm{MD} \tan\left(\frac{\Psi}{2}\right)}{\Psi}(\sin\phi_1 \cos\theta_1 + \sin\phi_2 \cos\theta_2) \tag{3.39}$$

$$\Delta \mathrm{E/W} = \frac{\Delta \mathrm{MD} \tan\left(\frac{\Psi}{2}\right)}{\Psi}(\sin\phi_1 \sin\theta_1 + \sin\phi_2 \sin\theta_2) \tag{3.40}$$

$$\Delta \mathrm{TVD} = \frac{\Delta \mathrm{MD} \tan\left(\frac{\Psi}{2}\right)}{\Psi}(\cos\phi_1 + \cos\phi_2) \tag{3.41}$$

where:

$$\Psi = 2\, a\cos\sqrt{\frac{1 + \cos\phi_1 \cos\phi_2 + \sin\phi_1 \sin\phi_2 \cos|\theta_1 - \theta_2|}{2}} \tag{3.42}$$

ΔMD = change in measured depth from station 1 to 2 (length), Ψ = angle subtended by circular arc (rad), ϕ_1 = inclination at station 1 (rad), ϕ_2 = inclination at station 2 (rad), θ_1 = azimuth at station 1 (rad), θ_2 = azimuth at station 2 (rad), ΔN/S = change in north or south coordinate from station 1 to 2 (length), ΔE/W = change in east or west coordinate from station 1 to 2 (length) and ΔN/S = change in true vertical depth from station 1 to 2 (length).

3.6
Sidewall Friction and Unconsolidated Drilling Issues

Sidewall friction affects all drilling operations. The sidewall friction of the drill string that is in contact with the steel casing or borehole wall in a vertical well is typically small. However, drilling operations in deviated, horizontal, and extended reach drilling (wells that are more than double in length than its true vertical depth) have frictional problems that limit the operations. Depending on the borehole trajectory and smoothness of the well in the curved and horizontal section of the borehole, significant additional drag forces or higher torques result. In many cases, no further drilling can occur, which is known as "lock-up."

This has stimulated considerable intensive research concerning sidewall friction. Prior to this time, most frictional work had been done in pile driving. Pile driving relies on sidewall friction to operate. Pile driving is related to a continuous penetrator. Both are driven by percussion hammer techniques.

3.6.1
Soil Penetration by Cones

Various penetrometer tests are run to determine the properties of soils. Despite the wide use of penetrometers, little work has been done on the theoretical basis of the operation. In general, when a penetrometer is driven into cohesionless soils, the soil is usually compacted by displacement and vibration. This develops a penetration resistance. The terms "penetration resistance" and "cone resistance" are strictly forces. However, these terms are often used to describe the force (static or dynamic) per unit base area of the cone required to push the cone into the soil (Poulos *et al.*, 1980). In addition, the penetrometer has to overcome the physical resistance in addition to the frictional resistance.

The frictional penetration resistance can be split into two main parameters: cone resistance and shaft friction (Bengough *et al.*, 1997). The cone resistance tends to decrease with increasing cone angle to a minimum at about 20–40° (Whitaker, 1976) and, thereafter, to increase (as shown in Figure 3.17). The cone resistance at small cone angles is associated with high soil–metal friction and, at large cone angles, with soil compaction ahead of the cone. As mentioned previously, a major control on the soil displacement is the cone angle. Soil tends to be displaced laterally at small cone angles, whereas the displacement becomes more vertical with increasing cone angles. In general, the amount of compaction near the tip is greater and the compaction near the shaft of the penetrometer is less.

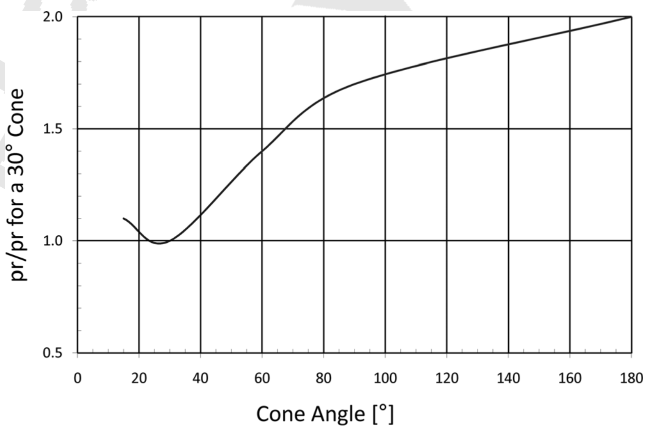

Figure 3.17 Cone angle versus cone resistance (Whitaker, 1976).

The downward movement of the penetrator relative to the surrounding soil also causes tangential forces on the shaft surface that oppose motion. These forces occur due to adhesion and friction of the soil on the shaft (Whitaker, 1976). In general, the shear stress averaged over the embedded penetrator shaft remains relatively constant below a critical depth.

The density of the soil also has a major effect. In very loose sands, soil movement extends 3–4 penetrometer diameters from the side of the borehole and 2.5–3.5 diameters below the penetrometer tip. In medium-dense sands, the extent of soil movement is larger, 4.5–5.5 diameters, and from the side 3–4.5 diameters below the tip. However, tests performed by Poulos and Davis (1980) showed that sand movements adjacent to the penetrometer sides follow the displacement and compaction of the sand at the penetrometer tip. These movements tend to decrease the sand density immediately around the penetrometer sides, equalizing the density increase effect of the tip compaction.

According to Poulos and Davis (1980), the diameter of the compacted zone around the penetrometer is seven times the diameter. Within this zone, the angle of friction, ϕ', changes linearly with the distance from the original value of ϕ'_1 at 3.5 times the radius to a maximum value of ϕ'_2 at the penetrator tip.

The relationship between ϕ'_1 and ϕ'_2 is as follows:

$$\varphi'_2 = \frac{\varphi'_1 + 40^\circ}{2} \tag{3.43}$$

3.6.2
Pile Driving Formulas

Pile driving formulas are derived by application of Newton's Second Law. By assuming that the materials of the pile and the driving cushion are perfectly elastic, and disregarding the inertia forces in the soil and energy losses stemming from irreversible deformations, the load capacity of the pile can be calculated. Because these conditions do not meet the letter of the law, their use can be questionable (Whitaker, 1976). Therefore, empirical constants and coefficients modify the pile driving formulas used today. Most of the practical pile driving formulas can be expressed in the following form:

$$e_{iv} e_f M H = \zeta \frac{1}{2}\left(\frac{R_u^2 L}{A_p Y}\right) + R_u S \tag{3.44}$$

where e_{iv} is the impact efficiency, e_f is the hammer impact efficiency, M is the hammer mass, H is the hammer drop distance, ζ is the elastic compression factor, R_u is the pile load bearing capacity, L is the pile length, A_p is the pile cross-sectional area, Y is Young's modulus, and S is the pile penetration distance for the previous impact.

The left-hand side of Equation (3.44) represents the energy of the hammer blow. The first term on the right-hand side is the energy consumed by the elastic compression of the pile (computed as a static compression under the force, R_u), and the second term is the energy absorbed by the plastic deformation of the soil.

This generalized representation of the pile driving formula can be applied towards a continuous penetrator. The difference would be that the pile now is actually a penetrator and that the load bearing capacity of the pile (maximum load before the soil fails in shear which is related to compressive strength) is the minimum load that must be applied for a further increase in depth of the penetrator.

The penetration resistance to the continuous penetrator is dependent only on ϕ, the angle of internal friction, and on the angle of external friction, ϕ_a. These angles can be calculated by application of the Mohr–Coulomb failure criterion. This can be developed by some simple triaxial tests on the materials to be penetrated.

If the slope of the line from a steel–soil interface on a Mohr–Coulomb chart is greater than the slope of the line from a soil test, then the soil meets the steel–soil failure criterion. The fractures created by the impact of the penetrator originate at the steel–soil interface. If the opposite slopes are true, then the soil meets the soil criterion. The fractures originate within the soil. No fractures will be created at the steel–soil interface and, therefore, no further penetration is possible. These tests give a qualitative result regarding the penetration ability of a penetrator in a particular soil and, therefore, the optimized penetration force.

Comparing the different practical driving formulas (around 450) with regard to accuracy between calculated data and actual field data, it is usually stated that the most accurate formula is Janbu's and is as follows (Poulos and Davis, 1980):

$$R_u = \left(\frac{1}{k_u}\right)\left(\frac{MH}{S}\right) \tag{3.45}$$

with

$$k_u = C_d\left(1 + \sqrt{1 + \lambda_l / C_d}\right) \tag{3.46}$$

$$C_d = 0.75 + 0.15\,\frac{M_p}{M} \tag{3.47}$$

$$\lambda_l = \frac{MHL}{A_p Y S^2} \tag{3.48}$$

where M_p is the pile mass (total mass of a continuous penetrator). Assuming that the mass of the hammer is close to the total mass of the penetrator, Equation (3.47) gives $C_d = 0.9$. Substituting Equations (3.48) and (3.47) into Equation (3.46) and substituting this result into Equation (3.45) gives

$$R_u = \frac{MH}{S\left(0.9 + 0.9\sqrt{1 + \frac{MHL}{0.9 \cdot A_p Y S^2}}\right)} \tag{3.49}$$

By rearranging the above equation, the term MH can be expressed as

$$MH = 0.1\, R_u\left(\frac{9LR_u}{A_p Y} + 18S\right) \tag{3.50}$$

If the force exerted by the impact of the hammer is close to the same in pile driving, the following statement can be made:

$$M\sqrt{2gH} = M_{\mathrm{PW}}\sqrt{2ah} \tag{3.51}$$

where g is the gravitational constant, M_{PW} is the pile mass, H is the pile dropping distance, h is the hammer striking distance, and a is the hammer acceleration.

The impact time is assumed to be similar and, therefore, cancels out. By rearranging Equation (3.51), the acceleration of the hammer can be calculated. Knowing the weight of the hammer and its striking distance, by substituting Equation (3.50) into Equation (3.51), one can derive the acceleration of the hammer:

$$a = \left[0.1\,R_{\mathrm{u}}\left(\frac{9LR_{\mathrm{u}}}{A_{\mathrm{p}}Y} + 18S\right)\frac{1}{M_{\mathrm{PW}}H}\right]^2 \frac{Hg}{h} \tag{3.52}$$

The evaluation of this equation gives a rough estimate of the acceleration necessary for further penetration. Because of the many assumptions made to derive Equation (3.52), the question of the accuracy is warranted. One major effect that is ignored is the vibrations created by the impact of the penetrator.

3.6.3 Methods of Cone Resistance Determination

Determining the acceleration for penetration, the cone resistance and shaft friction values should be as accurate as possible. This can be achieved by various methods. The most popular are the following:

- bearing capacity theory
- finite element methods
- numerical methods (wave equation)
- calibration chamber testing
- cavity expansion theory.

All of these methods correlate the cone resistance and engineering properties of soils. This correlation can be challenging because of the large strains and material non-linearity.

3.6.3.1 Bearing Capacity Theory

This particular theory is one of the first theories applied to the determination of penetration resistance. The penetration resistance is assumed to be equal to the collapse load of a deep circular foundation in soil. The bearing capacity theory uses two different approaches to determine the penetration resistance (Yu and Mitchell, 1998): limit equilibrium analysis and slip-line analysis.

3.6.3.1.1 **Limit Equilibrium Analysis** In this particular method, the failure criteria are initially assumed, then the failure load is determined by analyzing the global equilibrium of the entire soil mass. Depending on the failure criterion chosen, the results can be significantly different for the same conditions.

Although this analysis has often been applied because of its simplicity, the solutions obtained from this particular analysis are approximate. This does not model the effect of soil stress–strain behavior adequately. Another disadvantage is that shape factors must be used to convert from wedge to cone penetration. The determination of these shape factors causes an additional source of error.

3.6.3.1.2 **Slip-Line Analysis** In slip-line analysis, a yield criterion (similar to the Mohr–Coulomb criterion) is combined with the equations of equilibrium to derive a set of differential equations of plastic equilibrium in the soil mass. These differential equations can be used to construct a slip-line network from which a collapse load is determined.

Although this method takes into account the yield criterion and the equilibrium condition inside the slip line, its major disadvantage is that the stress distribution outside the slip line has no effect on the equations. In reality, the outside stresses do have an effect.

Regarding the bearing capacity theories overall, there are major limitations which need to be considered. First, the dependence of the penetration resistance on the stiffness and compressibility of the soil cannot be predicted since deformation of the soil is neglected. Second, this theory neglects the shaft resistance and states that the penetration resistance is the same as the resistance to the cone of the penetrator. The reality is that the horizontal stress tends to increase around the cone shaft after cone penetration. Third, the shear surfaces that are assumed for the bearing capacity method are usually not observed in a deep cone penetration.

3.6.3.1.3 **Finite Element Methods** Two different finite element methods model are used: the small strain and large strain models.

Small Strain Model In this model, the cone is placed into a prebored well with the surrounding soil still in its *in situ* stress state. By assuming that the collapse load is equal to the cone resistance, an incremental plastic collapse calculation is made. Because of the development of high lateral stresses next to the penetrator shaft during the penetration, the penetration resistance predicted by the small strain model is lower than in reality.

Large Strain Model The large strain model is used to incorporate the effects of cone penetration on the initial stress conditions. This is necessary because when the cone penetrates vertically into the soil, the result is a vertical displacement of several times the penetrator diameter. This large penetration effect is required to model the stress increase induced around the penetrator shaft.

Van den Berg *et al.* (1996), using an ALE (Arbitrary Lagrange Eulerean) algorithm, improved the large strain model. In this system, the movement of the element nodes and the material points is decoupled. Van den Berg *et al.* made the assumption that a steady state is reached when the penetration is about three times the penetrator diameter. The program used a standard elastoplastic model for the soil behavior, keeping the program simple. The implication is that the elastic segment of the deformations can be considered small with respect to the plastic segment. The finite element mesh is fixed in space; the material flows through it. The far-field effects have been modeled by the addition of spring elements at the outer boundary of the finite element model.

By rounding the cone shape, a smooth stress state is obtained around the corner point. Nevertheless, the assumptions and improvements of the model by Van den Berg *et al*. can cause severe numerical difficulties to arise (e.g., due to smoothing inherent to the convection algorithm). This is especially true for axisymmetric loading conditions. The accuracy of the calculated stresses from the finite element model is dramatically limited as the compressibility approaches zero. This phenomenon is called "locking" and has been observed by many researchers.

Using Van den Berg *et al*.'s finite element model, the calculated collapse load is about 23% higher than in reality. The numerical errors associated with the finite element analysis of cone penetration may be very significant. For this reason, finite element methods must be applied with caution.

3.6.3.2 Numerical Wave Methods

This approach models the pile driving system by a series of mass, spring, and sometimes damper elements. A wave is generated and is propagated through the model. The time during which the wave propagates is divided into small time steps. The reaction of each mass and spring is then calculated separately in every time step. The application of this approach allows the determination of stresses and of pile penetration against any penetration resistance (Smith, 1960).

The length of the elements and the time step value are limited by the wavelength being propagated. Generally, small values are needed in order "not to miss the wave" because the wave propagates through the element during the time step. This can lead to the use of an inordinate number of elements, and the subsequent difficulty and numerical instability of the solution. In this particular method, it is assumed that the soil compresses elastically for a certain distance (the "quake" factor, Q). It then fails plastically with a constant resistance, R_u.

Although this method can be very accurate, there is still a high possibility of errors due to an incomplete understanding of the behavior of soils during penetration. The results can differ significantly from the actual value of penetration resistance from the sensitivity of the solution to the damping factors. The choice of the damping factors is based on empirical experience and is subject to gross errors.

3.6.3.3 Calibration Chamber Testing

To be able to determine accurate, repeatable values for the penetration resistance of penetrators, large calibration chambers have been used for many years to establish empirical considerations between soil properties and penetration resistance. However, the results measured in the test chamber may differ from the actual values because the boundary conditions imposed in the chamber are not the same as those in the field. Depending on the displacements and stresses during the penetration the boundary conditions are in most cases one of the following (Yu and Mitchell, 1998):

- BC 1 – constant lateral and vertical stress
- BC 2 – vertical displacement and average lateral displacement zero
- BC 3 – constant vertical stress and average lateral displacement zero
- BC 4 – no vertical displacement and constant lateral stress.

The boundary condition effects of the chamber size would vanish if the chamber radius, B, approaches infinity (BC 1). This boundary condition is the more accurate condition for penetration under free field conditions.

Although chamber testing has been widely used to obtain correlations between penetration resistance and soil properties, there are limitations. First, correction factors must be applied to the chamber results in order to determine reliable results. This is because of the limited size of the calibration chambers. Second, in general, the soil stiffness is neglected in these tests. This can be improved by measuring the shear modulus directly in the individual chamber tests. Third, the results are valid only for the particular soil tested and are not transferable to any other type of soil.

3.6.3.4 **Cavity Expansion Theory**

When a penetrator penetrates soil, it first creates and then expands a cylindrical cavity. There is relationship between the penetration resistance and the pressure required to expand a cylindrical cavity from an initial zero radius. From different laboratory and field tests, during penetration of a continuous penetrator, a nearly conically shaped, rigid soil core is formed at the tip of the penetrator (Salgado *et al.*, 1997). The displacement field immediately below the tip, inside and along the soil core, is vertical. A rotation in the displacement field is observed from vertical underneath the penetrator to horizontal at some distance from the pile center. This horizontal displacement field is compatible with an expanding cylindrical cavity.

Two steps must be followed when using a cavity expansion analysis. They are to develop theoretical limit pressure solutions for cavity expansion in soils and to relate cavity expansion pressure to cone resistance.

In general, there are two cavity expansion problems. First, a cavity exists initially in the soil. The pressure in the cavity is in equilibrium with the stresses in the surrounding soil. In order to expand the cavity, an increasing pressure would be required. The cavity pressure approaches a limit when the cavity radius effectively approaches infinity. That means a steady-state pressure condition. Second, and opposite to the first problem, initially there is no cavity present in the soil. Any cavity expansion starts from a cavity radius of zero. Mathematically this is similar in approach to an expansion of an existing cavity to infinity. This means that the pressure created in a soil is equal to the steady-state cavity pressure.

Because a continuous penetrator creates a cylindrical cavity, penetration resistance is a function of steady-state cylindrical cavity pressure. The stress increase around the expanding cavity creates, depending on the induced strain levels, three different zones (Salgado *et al.*, 1997): a plastic, a non-linear elastic, and an elastic zone (Figure 3.18).

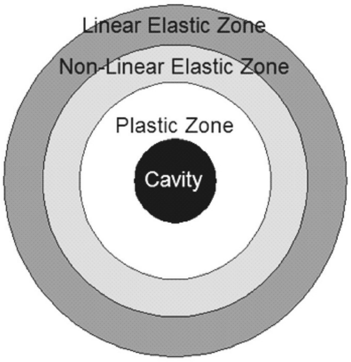

Figure 3.18 Cavity expansion zones.

3.6.3.4.1 **Plastic Zone** The stresses occurring in the plastic zone are large enough to cause failure of the soil in this zone. In this zone, the stress path followed by a soil element due to the expansion of a cavity in the soil is not the same as that one followed by a triaxial test sample. The mean effective stress of this sample, in contrast to what happens during cavity expansion, actually drops after the peak (Salgado *et al.*, 1997). In addition, variations in all quantities are acute near the cavity.

After computing stress values for the plastic zone, the limit pressure or the pressure in cavity when the ratio of the initial to the current cavity radius approaches zero can be calculated by the use of incremental steps for the plastic radius starting with small positive values:

$$p = \sigma_R \left(\frac{R}{a_c}\right)^{\frac{N-1}{N}} \tag{3.53}$$

where σ_R is the radial normal stress at the elastic–plastic interface, R is the inner radius of the elastic zone, which is equal to the outer radius of the plastic zone, a_c is the cavity radius, and N is the operative flow number.

The relationship between the radial normal stress and the limit cylindrical pressure and the relationship between the vertical stress along the cone and the penetration resistance can be determined:

$$\sigma_r = p_L \left(\frac{d_c}{2r}\right)^{\frac{N-1}{N}} \tag{3.54}$$

with

$$N = \frac{\ln\left(\frac{R}{a}\right)}{\frac{1}{N_m}\ln(R) - \frac{1}{N_1}\ln(a) + \sum_{i=1}^{m-1} n_i \ln(a + i\,t)} \tag{3.55}$$

where d_c is the cone diameter, N_1 is the element 1 flow number, and N_m is the mth element flow number.

The minimum vertical stress is reached at the penetrator tip where r_0 is zero. Accounting for the change in the vertical stress along the cone and the radial stress along the shaft, the penetration resistance to the continuous penetrator in a specific soil can be calculated. By using the penetration resistance, the optimum force and acceleration for further penetration can be determined. Using the Mohr–Coulomb failure criterion, this can be determined as follows:

$$F_{op} = F_{MCC} + F_{PR} \tag{3.56}$$

where F_{op} is the optimized penetration force, F_{MCC} is the Mohr–Coulomb steel–soil failure criterion force, and F_{PR} is the penetration resistance.

3.6.3.4.2 **Elastic Zone** In the non-linear elastic zone, the soil has yielded. The soil is in the non-linear stress-strain range. However, the stresses are not large enough for failure. This is considered a transition zone.

In the linear elastic zone, the strains are small enough that they do not cause any failure. Because an ideal cylindrical expansion takes place under plane strain conditions, there are no normal strains in the vertical direction; ε_z is zero. This region is visualized as an elastic hollow cylinder with inner radius, R, and outer radius, B, subjected to an internal pressure that increased from p_0 to the current radial normal stress, σ_R, at the inner radius.

Applying the Mohr–Coulomb failure criterion, the final expression for the stress field in the elastic zone is

$$\sigma_r - p_0 = \frac{N_p - 1}{N_p + 1} p_0 \frac{\left(\frac{R}{r}\right)^2 - \frac{N_p+1}{N_p-1}\gamma\left(\frac{R}{B}\right)^2}{1 + \gamma\left(\frac{R}{B}\right)^2} \tag{3.57}$$

and

$$\sigma_\theta - p_0 = -\frac{N_p - 1}{N_p + 1} p_0 \frac{\left(\frac{R}{r}\right)^2 + \frac{N_p+1}{N_p-1}\gamma\left(\frac{R}{B}\right)^2}{1 + \gamma\left(\frac{R}{B}\right)^2} \tag{3.58}$$

where

$$N_p = \tan^2\left(45 + \frac{\phi_p}{2}\right) \tag{3.59}$$

p_0 is the initial cavity pressure and is equal to the initial lateral stress, N_p is the peak flow number, r is the radius under investigation, γ is the boundary condition constant, σ_θ is the circumferential normal stress, and ϕ_p is the peak friction angle.

The cavity expansion approach has the advantages that both elastic and plastic deformations of the soil during cone penetration can be handled. In addition, this approach considers both the influence of the cone penetration process on the initial stress state and the effect of stress rotations that occur around the penetrator tip.

3.6.4
Pressure Bubble

During the penetration of a pile into a soil, a pressure bubble ahead of the end of the pile is created. The value of the pressure at a certain distance, z, ahead of the tip is dependent on the load applied (Craig, 1997) and is given by

$$\sigma_z = q\left\{1-\left[\frac{1}{1+\left(R_p/z_d\right)^2}\right]^{\frac{3}{2}}\right\} = I_c q \tag{3.60}$$

where σ_z is the stress (equal to pressure) at depth z_d, q is the applied axial load, R_p is the pile radius, and I_c is the influence factor.

The radial and circumferential stresses under the center are equal:

$$\sigma_r = \sigma_\theta = \frac{q}{2}\left\{(1+2\nu) - \frac{2(1+\nu)}{\left[1+(R/z)^2\right]^{\frac{1}{2}}} + \frac{1}{\left[1+(R/z)^2\right]^{\frac{3}{2}}}\right\} \tag{3.61}$$

where σ_r is the radial stress, σ_θ is the circumferential stress, and ν is Poisson's ratio. Figure 3.19 shows the influence factor I_c versus terms of D/z. The curve shows that with increasing depth z (which decreases the ratio D/z for constant D), the influence factor I_c decreases. The result is that the greater the distance ahead of the tip, the lower is the pressure.

This is applicable to a continuous penetrator. During the penetration of the tip into a soil, a pressure bubble is also created ahead of the tip (Craig, 1997). In comparison with the results for a pile, the stress is higher because of the smaller surface area. This will not change the influence factor decrease with depth. The pressure at a given

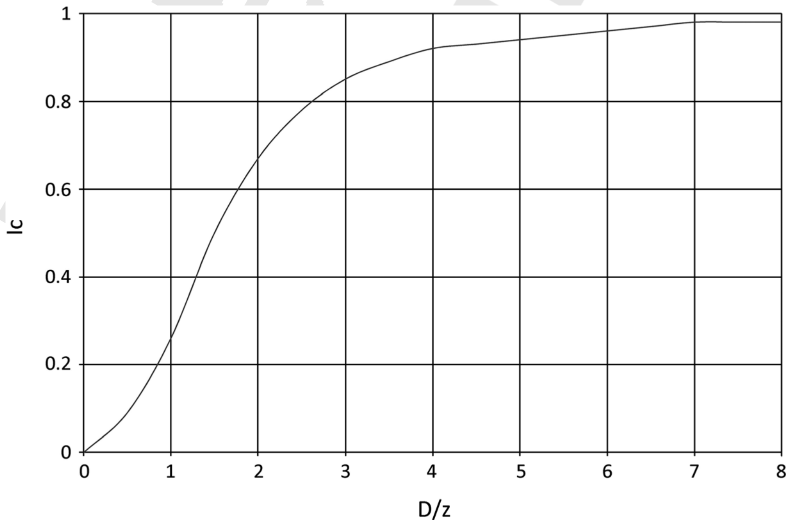

Figure 3.19 Distribution of the pressure bubble influence factor in relation to depth.

depth below the tip will be higher because of the same applied load over a smaller area. However, the influence factor I_c will remain the same. In general, it appears that the pressure bubble is too small to create additional fractures in the soil, assuming that the force at the tip of the penetrator is optimized for penetration.

3.6.5 Permafrost Piling

Standard penetration tests have been performed in fine-grained soils to a temperature of $-3\,°C$ (26.6 °F) and into coarse-grained soils to $-1\,°C$ (30.2 °F). The penetration resistance increases steeply with decreasing temperature. In soils at temperatures lower than $-3\,°C$, piles are driven by drilling a pilot hole. This reduces the driving stresses and pile installation time. In general, piles can be driven in most frozen soils (except frozen gravels and cobbles) with impact, vibratory, or sonic hammers.

Three major forces are predominant regarding the penetration resistance in permafrost (Charest *et al.*, 1963): the crushing, the drag, and the friction force. These three forces have associated with them three decelerations: crushing, drag, and frictional deceleration, respectively (Nottingham and Christopherson, 1983).

Crushing forces and drag forces are present at the initiation of penetration. The crush forces are the minimum forces necessary to penetrate the permafrost and permit the pile to be driven into the ground. The drag forces are the forces necessary to accelerate the crushed permafrost particles out of the way. The friction forces act along the side of the penetrator and increase with increasing penetration until the penetrator is completely buried.

The penetration resistance to a continuous penetrator in permafrost is considered to be larger than in a regular soil because permafrost is a kind of consolidated soil.

A problem in permafrost penetration is the occurrence of freeze-back pressure. Freeze-back can occur within minutes to hours. The freeze-back pressure can be significantly high and varies with the temperature.

3.6.6 Vibratory Pile Driving

Vibratory pile driving is an alternative pile installation technique. The piles are attached to a vibrator and driven into the ground by vertical vibrations. The major advantages of this technique are faster rates of penetration and a significant decrease in the shaft frictional resistance (Dufour *et al.*, 1983).

Vibratory pile driving is mainly influenced by the following parameters (Vipulanandan *et al.*, 1990):

- vibrator peak acceleration
- displacement amplitude
- frequency
- non-inertia load (bias weight)
- pile cross-sectional area
- soil grain size

- angle of internal friction
- shaft resistance.

By driving the pile at a second harmonic resonant frequency, good results were achieved, even in permafrost where conventional impact driving often leads to excessive pile damage (O'Neill *et al.*, 1990). The optimum driving frequency is independent of grain size, relative density, mean *in situ* effective stress, and bias weight.

During vibratory pile driving, the pile sinks as though it were in a highly viscous fluid. This is conjectured to be because the soil is fluidized. Fluidization is the action of soil particles when excited by a vibrational source of the proper frequency. During this excitement, the granular soil is transformed into a fluid-like state that offers little resistance to movement of bodies through the medium. Soil systems do not have a specific natural frequency but instead have a natural frequency spectrum. Rodger and Littlejohn (1980) gave different natural frequency ranges for unfrozen soils depending on the grain size:

- coarse-grained soils: 4–10 Hz
- fine–medium-grained sands: 10–40 Hz
- cohesive soils: 40–100 Hz.

They further give recommendations on how to handle vibratory pile driving in the different soil types.

Figure 3.20 shows a natural response spectrum of soil that was recorded in Taft, CA, on 21 July, 1952 (Wiegel *et al.*, 1970). The figure shows the range for the natural frequency of this soil.

The ROP while vibratory pile driving changes with depth and the bias mass force. The lateral effective soil pressure (sidewall friction) has a greater influence on this

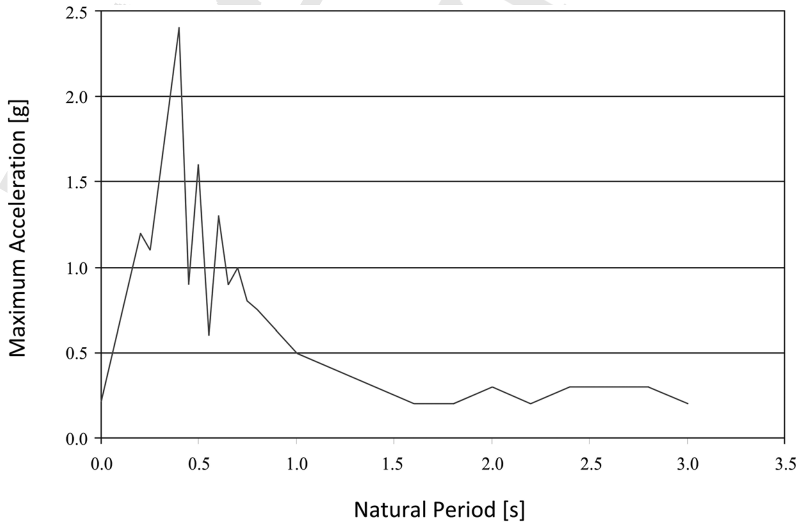

Figure 3.20 Soil natural frequency response spectrum (Wiegel *et al.*, 1970).

effect than the vertical effective pressure (cone resistance) (Crory, 1982). In general, the sidewall friction is reduced with respect to the normal friction value. This can be explained by examining the Poisson's ratio.

A driven pile will undergo vibrations of alternating compressive and tensile forces from the longitudinal waves created along its axis. The pile diameter will expand and contract synchronously with the applied tensile and compressive stress waves. For short durations during a vibration cycle, the pile may be physically free of contact with the soil. Because of this effect and the liquefaction of soil, the shaft friction is reduced to a small fraction of the static friction value. Accelerations of a few *g* will reduce friction levels to almost one-third of their static value.

The energy required for vibratory pile driving depends strongly on the relative density of the soil. Less energy is needed for vibratory pile driving compared with impact driving at a relative density of 65%. At a relative density of 90%, vibratory pile driving consumes three to eight times more energy than impact driving. Hence vibratory pile driving may not always be more efficient than impact driving from an energy consumption perspective.

Driving piles by a vibrator into permafrost has additional benefits. For example, melting of permafrost was observed around the pile during the driving operation. This observation may mean that the penetration into the permafrost is a consequence of soil melting at the tip. As the frequency of the pile driver achieves resonance, the pile transmits the driving energy efficiently to the tip and produces an overall heating of the pile. This produces a thin thawed zone around the pile, which is fluidized by the vibrations of the pile, permitting it virtually to slip into or out of the frozen ground.

However, the freezeback is relatively rapid (minutes to hours) and the corresponding freeze bond strength is high. The advantage of resonant vibratory pile driving is that it can transform mechanical energy into thermal energy.

The thawed zone produced in tests with a pile of 25.4 mm outer diameter varied from 1.5 to 2.5 mm. The average temperature recorded at the film–pile interface was $+2\,^{\circ}$C (maximum $+4\,^{\circ}$C). However, there was no disturbance of the soil ahead of the pile tip. The thawed zone was contaminated by steel dust produced by the abrasive action of the thawed soil on the oscillating model pile.

Frequency is the most critical parameter in vibratory pile driving. A frequency exists below which no further penetration is possible because the bias surcharge becomes too high for the displacement amplitude. As the frequency decreases, the displacement increases but the acceleration decreases. There is also an upper threshold frequency above which no penetration will be possible because displacements at frequencies higher than this particular threshold frequency are too small to allow for transfer of sufficient energy to the soil and as a result the pile will not penetrate.

3.6.7
Impact on Penetration Resistance

The previously listed parameters have a large effect on the penetration resistance. Some of these effects increase the penetration resistance, whereas others decrease it.

The primary effects, such as angle of friction, cone angle, and cohesion, have been discussed previously in this section. Other effects are:

- soil type
- water content
- rotation of the penetrator
- soil temperature
- matrix pressure
- cone roughness.

3.6.7.1 Soil Type

The important soil type variables include bulk density, texture, particle shape, mineralogy, amorphous oxide content, organic matter content, and chemical composition of the soil solution (Bourgoyne *et al.*, 1986). The cone resistance increases with increasing bulk density of the soil. The shape of sand particles may influence cone resistance through their influence on both soil internal friction and soil–metal friction.

The effective stress is related to matrix potential and the pore size distributions, which influence cone resistance. Calcium carbonate encourages soil aggregation whereas an excess of sodium leads to slaking. Cone resistance was found to increase with the calcium carbonate content in fine-grained soils.

3.6.7.2 Water Content

Cone resistance decreases with increasing soil water content or matrix potential. The matrix potential and the water content may change during penetration because of soil compression and particle rearrangement, where as gravimetric water content remains constant. The rate of change of resistance with water content is less at low than at high bulk density (Smith and Mullins, 1991).

The presence of water or fluid influences the shaft friction. In petroleum drilling operations, the friction between the drill string and the casing and also between the drill string and the formation is decreased by the use of drilling mud. The build-up of a fluid film between the two elements helps to lubricate the contact. This fluid film development can be achieved during penetration of permafrost from the creation of water as described in Section 3.6.6.

3.6.7.3 Rotation of the Penetrator

By rotating the continuous penetrator, the penetration resistance can be decreased by over a half, on both the tip and the shaft. This was proven also by tests run in rotary drilling. The additional drag and torque during tripping in a horizontal well are less if the drill string is rotated. If the penetrator rotates, the angle at which the resultant stress acts also changes.

3.6.7.4 Soil Temperature

The penetration rate generally decreases as the soil temperature is lowered. This is because strength increases with decreasing temperature (Mirreh and Ketcheson, 1991).

Depending on a combination of parameters, the soil can inhibit plastic deformation, which greatly inhibits the ROP.

3.6.7.5 Matrix Pressure

The matrix pressure will generate a friction force. The friction force rises with increase in matrix pressure. Clays present in permafrost can increase the matrix pressure because of clay swelling upon contact with the water created by the penetration process (Mirreh and Ketcheson, 1972).

3.6.7.6 Cone Roughness

Rough cones increase the penetration resistance, whereas smooth cones decrease it. This effect does not have a significant influence because rough cones become smooth after a couple of meters of penetration due to the abrasiveness of the soil.

3.7 Conclusion

In this chapter, the basics of ground drilling and excavation have been reviewed. The types of drilling rigs used on Earth were reviewed. These included the percussion drilling rig and the rotary drilling rig. Also reviewed were the subsystems and related basic power and volume calculations needed for drilling.

There are three things to be accomplished:

- penetration of the material
- removal of the material
- maintaining the borehole stability.

Penetrating the material is accomplished by either by drilling with a bit and the associated equipment that supports the bit. The drilling process can be by melting and vaporization, thermal spallation, chemical reactions, or mechanical breakage. Of these, mechanical breakage is the overwhelming choice for drilling soils and rocks. There are two mechanical methods of drilling: percussion and rotary. Percussion impacts the rock or soil perpendicularly and the rotary method either shears or crushes the rock or soil. Mechanical drilling can also be a combination of the two methods.

Removing the material, also known as cuttings transport, involves cleaning under the bit and moving the material out of the borehole. There are only two methods for doing this: either using fluids such as pneumatic, liquid, or a combination, or mechanical means such as an auger. It is best to remove the material from the borehole as recompaction of the cut material is difficult to achieve.

Supporting the borehole is as simple as a borehole fluid exerting a hydrostatic pressure to maintain the borehole stability. Or maintaining borehole stability could be as complex as lowering a steel pipe into the borehole and cementing it *in situ*. The design of the steel pipe can be found in numerous drilling textbooks.

Another issue in drilling is directional control. Directional control is affected by geology, rock properties, borehole conditions, the bit design, and the bottom hole assembly. The two methods for controlling the bit are either to tilt the bit or to push the bit in the desired direction. Usually it is a combination of the two controlling processes that determines the direction of the borehole.

Unconsolidated soil drilling and sidewall friction have other issues. Pushing a bit into the soil can be challenging but successful, depending on the nature of the soil. Many methods described in this chapter have been developed to determine the success of soil penetration and the resulting friction factors. These friction factors will also affect directional control and the application of energy at the bit.

Acknowledgments

The authors acknowledge the efforts of the reviewers for this chapter and appreciate their efforts to improve the content. The reviewers include:

- Brian Tarr – Deepwater Well Technology, Shell International Exploration and Production Inc., Houston, TX
- Lou Capuano – Chief Executive, Thermasource, Santa Rosa, CA
- Sam Abraham – Geothermal Resource Group Inc., Palm Desert, CA
- William M Rickard – President, Geothermal Resource Group Inc., Palm Desert, CA
- Doug Blankenship and his group – Sandia National Laboratories, Albuquerque, NM
- Roy Long – E&P Technology Manager, Strategic Center for Natural Gas & Oil, DOE/National Energy Technology Laboratory, Tulsa, OK
- Robert Mitchell – Fellow, Halliburton Drilling and Evaluation Division, Houston, TX.

The authors also acknowledge:

- Nic Nickels – Baker Hughes, Houston, TX, for recommending reviewers
- Bobby Grimes – Hughes Christensen, The Woodlands, TX, for his help in securing photographs
- Brian Wilcox – Jet Propulsion Laboratory, Pasadena, CA, for his support for the original reports to the JPL upon which this chapter is based.

References

American Petroleum Institute (1998) Recommended Practice for Drill Stem Design and Operating Limits, API RP 7G, 16th edn, December 1998.

Appl, F.C. and Rowley, D.S. (1968) Analysis of surface set diamond bit performance. Proceedings of the 43rd Fall Meeting in Houston, TX, 29 September 29–2 October 1968, SPE 2242.

Atkinson, B.K. (1987) *Fracture Mechanics of Rock*, Academic Press, Harcourt Brace Jovanovich, San Diego, CA.

Azar, J.J. and Samuel, G.R. (2007) *Drilling Engineering*, Pennwell, Tulsa, OK.

Baird, J.A., Caskey, B.C., Tinianow, M.A. and Stone, C.M. (1984) GEODYN, A geological formation/drilling dynamics computer program. 59th Annual Fall Conference and Exhibition of the SPE, Houston, TX.

Bažant, Z.P. (1985) In *Mechanics of Geomaterials: Rocks, Concretes, Soils* (eds R.H. Gallagher and O.C. Zienkiewicz), Wiley Series in Numerical Methods in Engineering, John Wiley & Sons, Inc., New York, p. 611.

Bengough, A.G. *et al.* (1997) Estimating soil frictional resistance to metal probes and its relevance to the penetration of soil by roots. *European Journal of Soil Science*, **48**, 603–612.

Birades, M. and Fenoul, R. (1986) ORPHEE 2D: a microcomputer program for prediction of bottomhole assembly trajectory. Symposium on Petroleum Industry Application of Microcomputers of the SPE, Silvercreek, CO.

Boart Longyear (2008) Sonic drilling.pdf, http://www.geotechinc.com/equip_rotosonicdrilling.html (accessed 8 January 2009).

Q8 Bogy, D.B. and Pasley, P.R. (1964) Buckling of drillpipe in an inclined hole. *Journal of Engineering for Industry, Transactions of the ASME*.

Bourgoyne, A.T., Chenevert, M.E., Millheim, K.K. and Young, F.S. (1986) *Applied Drilling Engineering*, SPE Textbook Series, **2**, Society of Petroleum Engineers, Richardson, TX.

Brady, B.H.G. and Brown, E.T. (1992) *Rock Mechanics for Underground Mining*, 2nd edn, Chapman & Hall, London.

Q9 Brakel, J.D. and Azar, J.J. (1989) Prediction of borehole trajectory considering bottomhole assembly and drill-bit. *Dynamics. SPE Drilling Engineering*.

Brantly, J.E. (1971) *History of Oil Well Drilling*, Gulf Publishing, Houston, TX.

Brett, J.F., Gray, J.A., Bell, R.K. and Dunbar, M.E. (1986) A method of modeling the directional behavior of bottomhole assemblies including those with bent subs and downhole motors. Drilling Conference of the IADC/SPE, Dallas, TX.

Bridgford, E., Tischler, A. and Eustes, A. (2000) Force penetration values for permafrost in relation to the Mars subsurface explorer. Energy Sources Technology Conference/Offshore Mechanics and Arctic Engineering 2000 Conference, New Orleans, LA, 14 February 2000. Q7

Bruce, W.E. *et al.* (1969) Drillability Studies – Laboratory Percussive Drilling, USBM Report of Investigation 7300.

Cerkovnik, F. J. (1998) Directional/MWD. Seminar, Baker Hughes Inteq, Golden, CO.

Charest, J. *et al.* (1963) Model studies of rapid driving of piles into permafrost. Paper SPE 497, presented at the Drilling and Rock Mechanics Conference, Austin, TX, 23–24 January 1963.

Chen, W.F. and Saleeb, A.F. (1982) *Constitutive Equations for Engineering Materials*, vol. **1**, John Wiley & Sons, Inc., New York.

Clark, G.B. (1979) Principles of rock drilling. *Colorado School of Mines Quarterly*, **74** (2). Q10

Craig, R.F. (1997) *Soil Mechanics*, 6th edn, E & FN Spon, London.

Crory, F.E. (1982) Piling in frozen ground. *Journal of the Technical Counsels of ASCE*, **108** (TCI). Q11

David, C., Menéndez, B. and Bernabé, Y. (1998) The mechanical behaviour of synthetic sandstone with varying brittle cement content. *International Journal of Rock Mechanics and Mining Sciences*, **35** (6). Q12

Desai, C.S. and Siriwardane, H.J. (1984) *Constitutive Laws for Engineering Materials*, Rainbow-Bridge Book Co., Taiwan

Dufour, S. *et al.* (1983) Vibratory model pile driving in frozen sand. Proceedings of the 4th International Conference for Permafrost, Fairbanks, AK, 17–22 July, 1983.

Dunnigan, J.F. (1999) *Dirty Little Secrets of the Twentieth Century*, William Morrow, New York.

Dvorkin, J., Mavko, G. and Nur, A. (1991) The effect of cementation on the elastic properties of granular materials. *Mechanics of Materials*, **12**. Q13

Q14 Dvorkin, J., Yin, J. and Nur, A. (1994) Effective properties of cemented granular materials. *Mechanics of Materials*, **18**.

Q15 Enen, J., Callas, N.P. and Sullivan, W. (1984) Rig site computer optimizes bit weight against hole angle for bottom-hole assemblies. *Oil and Gas Journal*.

Eustes, A.W. (2007) The evolution of automation in drilling. SPE Annual Technical Conference and Exhibition, Anaheim, CA, 11–14 November 2007.

Eustes, A.W. and Stoner, M.S. (1999) Directional Control of the Subsurface Explorer Report in Support of the Martian Subsurface Explorer, Colorado School of Mines report to the Jet Propulsion Laboratory.

Q16 Eustes, A.W., Mitchell, B.J. and Stoner, M.S. (1994) Selection of slim hole core rods by vibratory analysis. *Journal of Energy Resources Technology*.

Eustes, A.W., Mitchell, B.J. and Long, R.C. (1995) Core bit frequency signatures. ASME Energy Sources Technology Conference and Exhibition, Houston, TX.

Eustes, A.W., Gertsch, L.S., Lu, N., Stoner, M.S., Tischler, A. and Bridgford, E. (1999) Summary of Drilling Research in Support of the Martian Subsurface Explorer, Colorado School of Mines report to the Jet Propulsion Laboratory.

Eustes, A.W., Gertsch, L.S., Lu, N., Bridgford, E., Tischler, A., Stoner, M.S. and Wilcox, B.H. (2000) Summary of Issues Regarding the Martian Subsurface Explorer, Space Resources Roundtable II.

Gantt, L.L. *et al.* (1998) Coiled tubing drilling on the Alaskan North Slope, Oilfield Review, Summer, Schlumberger.

Graff, K.F. (1979) Ultrasonic comminution. Proceedings of Ultrasonics International 1979, Austria.

Guéguen, Y. and Palciauskas, V. (1994) *Introduction to the Physics of Rocks*, Princeton University Press, Princeton, NJ.

Q17 Hartman, H.L. (1959) Basic studies of percussive drilling. *Mining Engineering*, **11**.

Heisig, G., Oppelt, J., Neubert, M. and Donati, F. (1996) Closed-loop guided directional drilling fundamentals, concepts, and simulations. Energy Week Drilling Technology Symposium of the ASME, Houston, TX.

Hightower, C.M. and Blount, C.G. (1998) An operator coiled tubing drilling history. World Oil's 6th International Coiled Tubing and Well Intervention Conference and Exhibition, Houston, TX, 9–11 February 1998.

Ho, H.S. (1986) General formulation of drillstring under large deformation and its use in BHA analysis. 61st Annual Fall Conference and Exhibition of the SPE, New Orleans, LA.

Hoch, R.S. (1962) A Review of the Crooked-Hole Problem and an Analysis of Packed Bottom-Hole Drill-Collar Assemblies, API Drilling and Production Practices.

Hock, E. and Brown, E.T. (1982) *Underground Excavations in Rock*, Institute of Mining and Metallurgy, London.

Hoffmann, J.I. (1912) Recent practice in diamond drilling and borehole surveying. *Transactions of the Institution of Mining and Metallurgy*, **21**. Q18

Hustrulid, W.A. and Fairhurst, C. (1971) A theoretical and experimental study of the percussive drilling of rock. *International Journal of Rock Mechanics*, **8**. Q19

Hycalog (1994) PDC Bit Technology Manual, Hycalog.

ICoTA (2005) An Introduction to Coiled Tubing – History, Applications and Benefits, ICoTA, Longview, TX; http://www.icota.com/publications.

Jaeger, H.M. (1997) Chicago experiments on convection, compaction, and compression. Proceedings of the NATO/ASI Workshop on Dry Granular Materials, Cargese, preprint.

Jeremic, M.L. (1987) *Ground Mechanics in Hard Rock Mining*, Balkema, Rotterdam.

Jimeno, C.L., Jimeno, E.L. and Francisco, J.A.C. (1995) *Drilling and Blasting of Rocks*, Balkema, Rotterdam.

Jogi, P.N., Burgess, T.M. and Bowling, J.P. (1986) Three-dimensional bottomhole assembly model improves directional drilling. Drilling Conference of the IADC/SPE, Dallas, TX.

Q20 Kim, D.S. and Drabkin, S. (1995) Investigation of vibration-induced settlement using multifactorial experimental design. *Geotechnical Testing Journal*, **18**.

Q21 Knight, J.G., Ehrichs, E.E., Kuperman, V.Yu., Flint, J.K., Jaeger, H.M. and Nagel, S.R. (1996) Experimental study of granular convection. *Physical Review E*, **54** (5).

Koper, M.G. and Fowler, M. (1999) The Galileo experience. SPE/IADC 57570, SPE/IADC Middle East Drilling Technology Conference, Abu Dhabi, UAE, 8–10 November 1999.

Lo, Y.C. and Herbst, J.A. (1990) Comminution alternatives of effective production in fine particles. 7th European Symp on Comminution, Yugoslavia.

Lo, Y.C. and Kientzler, P. (1992) Evaluation of the effectiveness of ultrasonic comminution. in *Comminution – Theory and Practice, SME/AIME Symposium* (ed. S. Komar Kawatra), Society for Mining, Metallurgy, and Exploration, Littleton, CO, Chapter 9.

Q22 Long, R.C. and Mitchell, B.J. (1992) A new approach to directional survey interpretation and course correction by the sectional method. *Journal of Energy Resources Technology*.

Q23 Lundberg, B. (1973) Energy transfer in percussive rock destruction. *International Journal of Rock Mechanics*, **10**.

Lyons, W.C., Guo, B. and Seifel, F.A. (2001) *Air and Gas Drilling Manual*, McGraw-Hill, New York

Q24 Ma, D. and Azar, J.J. (1986) A study of rock–bit interaction and borehole deviation. *Journal of Energy Resources Technology*.

Maurer, W. (1968) *Novel Drilling Techniques*, Pergamon Press, Oxford

Maurer, W. (1980) *Advanced Drilling Techniques*, Petroleum Publishing Company, Tulsa, OK

Q25 McLamore, R.T. (1971) The role of rock strength anisotropy in natural hole deviation. *Journal of Petroleum Technology*.

McLennan, J., Carden, R.S., Curry, D., Stone, C.R. and Wyman, R.E. (1997) *Underbalanced Drilling Manual*, Gas Research Institute, Chicago, IL.

NETL (2005a) Coiled Tubing, State of the Industry and Role for NETL, US DOE – Office of Fossil Energy, NETL, June 2005.

NETL (2005b) Microhole Technology, US DOE – Office of Fossil Energy, NETL, October 2005.

Millheim, K.K. (1977) The effect of hole curvature on the trajectory of a borehole. 52nd Annual Fall Technical Conference and Exhibition of the SPE, Denver, CO.

Millheim, K.K. (1978a) Here are the basics of bottom-hole assembly mechanics. *Oil and Gas Journal*. Q26

Millheim, K.K. (1978b) Operators have much to learn about directional drilling. *Oil and Gas Journal*. Q27

Millheim, K.K. (1978c) Proper application of directional tools key to success. *Oil and Gas Journal*. Q28

Millheim, K.K. (1978d) Single-stabilizer behavior described. *Oil and Gas Journal*. Q29

Millheim, K.K. (1979a) Behavior of multiple-stabilizer bottom-hole assemblies. *Oil and Gas Journal*. Q30

Millheim, K.K. (1979b) Control techniques for medium-soft and medium formations. *Oil and Gas Journal*. Q31

Millheim, K.K. (1979c) Controlling hole direction in very soft formations. *Oil and Gas Journal*. Q32

Millheim, K.K. (1979d) Hard-formation directional drilling calls for special care. *Oil and Gas Journal*. Q33

Millheim, K.K. and Apostal, M.C. (1981) The effect of assembly dynamics of the trajectory of a bit. *Journal of Petroleum Technology*. Q34

Millheim, K.K., Jordan, S. and Ritter, C.J. (1978) Bottom-hole assembly analysis using the finite-element method. *Journal of Petroleum Technology*. Q35

Mitchell, B.J. (1995) *Advanced Oilwell Drilling Engineering Handbook*, Mitchell Engineering, Golden, CO.

Murphey, C.E. and Cheatham, J.B.J. (1965) Hole deviation and drill string behavior. *Society of Petroleum Engineers Journal*. Q36

Neubert, M. and Heisig, G. (1997) Advanced trajectory simulation of directional boreholes. Energy Week Drilling Technology Symposium of the ASME, Houston, TX.

Newman, K. (2004) Developments in coiled tubing technology. West Coast PTTC Workshop, Valencia, CA, 21 October 2004.

Nottingham, D. and Christopherson, A.B. (1983) Driven piles in permafrost: state of art. Proceedings of the 4th International Conference for Permafrost, Fairbanks, AK, 17–22 July 1983.

Q37 O'Neill, M.W. *et al.* (1990) Laboratory modeling of vibro-driven piles. *Journal of Geotechnical Engineering*, **116** (8), 1,190–1.

Q38 Perry, J. (1992) A technique for defining non-linear shear strength envelopes, and their incorporation in a slope stability method of analysis. *Quarterly Journal of Engineering Geology*, **27**.

Poulos, H.G. and Davis, E.H. (1980) *Pile Foundation Analysis and Design*, John Wiley & Sons, Inc., New York.

Prasher, C.L. (1987) *Crushing and Grinding Process Handbook*, John Wiley & Sons, Inc., New York.

Rafie, S. (1988) Mechanistic approach in designing BHA's and forecasting borehole position. Drilling Conference of the IADC/SPE, Dallas, TX.

Q39 Rémond, S. (2003) Simulation of the compaction of confined mono-sized spherical particles systems under symmetric vibration. *Physica A*, **329**.

Q40 Rodger, A.A. and Littlejohn, G.S. (1980) A study of vibratory driving in granular soils. *Geotechnique*, **30** (3).

Q41 Salgado, R. *et al.* (1997) Cavity expansion and penetration resistance in sand. *Journal of Geotechnical and Geoenvironmental Engineering*, **123** (4).

Schlecht, M. (1999) *Directional Drilling. An Overview Seminar*, Baker Hughes Inteq, Houston, TX.

Q42 Sifferman, T.R., Meyers, G.M., Haden, E.L. and Wahl, H.A. (1974) Drill cutting transport if full-scale vertical annuli. *Journal of Petroleum Technology*.

Simon, R. (1963) Energy balance in rock drilling. Proceedings of the SPE Texas Drilling and Rock Mechanics Symposium, Austin TX, January, SPE 999.

Simon, R. (1964) Transfer of the stress wave energy in the drill steel of a percussive drill to the rock. *International Journal of Rock Mechanics*, **1**. Q43

Smith, E.A.L. (1960) Pile-driving by the wave equation. *Journal of Soil Mechanics and Foundations Division*, **86** (SM 4). Q44

Smith, K.A. and Mullins, C.E. (1991) *Soil Analysis – Physical Methods*, Marcel Dekker, New York.

Spanos, P.D. and Payne, M.L. (1992) Advances in dynamic bottomhole assembly modeling and dynamic response determination. Drilling Conference of the IADC/SPE, New Orleans, LA.

Swanson, G.J. (1994) Rotasonic revisited: is there a production breakthrough in its future? *Water Well Journal*. Q45

Tarbuck, E.J. and Lutgens, F.K. (1999) *Earth, an Introduction to Physical Geology*, Prentice Hall, Upper Saddle River, NJ.

Teale, R. (1965) The concept of specific energy in rock drilling. *International Journal of Rock Mechanics*, **2**. Q46

Tischler, A., Eustes, A.W. and Gertsch, L.S. (1999a) Drilling Energy Report in Support of the Martian Subsurface Explorer, Colorado School of Mines report to the Jet Propulsion Laboratory.

Tischler, A., Eustes, A.W. and Lu, N. (1999b) Sidewall Friction Report in Support of the Martian Subsurface Explorer, Colorado School of Mines report to the Jet Propulsion Laboratory.

Toutain, P. (1981) Analyzing drill string behavior: Part 1 – an introduction to deviation control parameters. *World Oil*. Q47

Tsytovich, N.A. (1975) *The Mechanics of Frozen Ground*, McGraw-Hill, New York.

Van den Berg, P. *et al.* (1996) An Eulerean finite element model for penetration in layered soil. *International Journal for Numerical and Analytical Methods, in Geomechanics*, **20**. Q48

Vipulanandan, C. *et al.* (1990) Behavior of vibro driven piles in sand. *Journal of Geotechnical Engineering*, **116** (8). Q49

Q50 Walker, B.H. (1973) Some technical and economic aspects of stabilizer placement. *Journal of Petroleum Technology*.

Q51 Walstrom, J.E. (1969) An analysis of uncertainty in directional surveying. *Journal of Petroleum Technology*.

Whitaker, T. (1976) *The Design of Piled Formations*, 2nd edn, Pergamon Press, New York.

Q52 White, E.E. (1912) Surveying and sampling diamond-drill holes. *Transactions of the American Institute of Mining Engineers*, **44**.

Wiegel, R. *et al.* (1970) *Earthquake Engineering*, Prentice-Hall, Englewood Cliffs, NJ.

Williams, J. (1998) Bottom Hole Assembly Design and Guidelines Seminar, Parker Drilling Company, American Association of Drilling Engineers, Denver, CO.

Williamson, H.S. (1999) Accuracy prediction for directional MWD. SPE Annual Conference and Exhibition, Houston, TX.

Williamson, J.S. and Lubinski, A. (1986) Predicting Bottom-hole Assembly Performance, SPE Paper Number 14764.

Wills, B.A. (1997) *Mineral Processing Technology*, Butterworth Heinemann, Oxford.

Wolf, C.M. and deWardt, J.P. (1981) Borehole position uncertainty – analysis of measuring methods and derivation of systematic error mode. *Journal of Petroleum Technology*. Q53

Yu, S.H. and Mitchell, J.K. (1998) Analysis of cone resistance: review of methods. *Journal of Geotechnical and Geoenvironmental Engineering*, **124** (2). Q54

Zang, A. and Wong, T.F. (1995) Elastic stiffness and stress concentration in cemented granular material. *Int J Rock Mech Geomech, Abstr*, **32**. Q55

Keywords/Abstract

Dear Author,

Please check and/or supply keywords and an abstract. These will not be included in the print version of your chapter but in the online version.

If you do not supply an abstract, the section heading will be used instead.

Keywords: drilling; excavation; drilling rigs; cuttings removal; directional drilling; sidewall friction; pile driving; penetration resistance.

Author Query

1. The references Simon, 1958; Besson et al., 2001; Pang et al., 1986; Mitchell, 1992; Lyons, 2000; Wills, 1992; Rafie, Ho and Chandra, 1986; Mirreh and Ketcheson, 1991; Mirreh and Ketcheson, 1972 are cited in the text but not listed among the references. Please supply full references, or the citations will be deleted from the text.
2. There is no chapter with a title of or near "Rock Properties". Please give the full chapter title and the authors so we can identify it.
3. There is only one 1964 reference in the Ref. list, not 1964a and 1964b. Please clarify.
4. Fischer 1974: not in the Ref. list.
5. Walker and Friedman 1977: not in the Ref. list.
6. Callas 1981: not in the Ref. list.
7. References [ICoTA, 2005; Bridgford et al., 2000; NETL, 2005a; Eustes et al., 1999; Eustes et al., 2000; Eustes and Stoner, 1999; Gantt et al., 1998; Hightower and Blount, 1998; Koper and Fowler, 1999; Lyons et al., 2001; NETL, 2005b; Newman, 2004; Simon, 1963; Teale, 1965; Tischler et al., 1999a, Tischler et al., 1999b, Williamson and Lubinski, 1986; Wills, 1997] are not cited in the text. Please cite them in the text or remove them form the reference list.
8. Please provide the Volume and page range in ref. (Bogey and Pasley, 1964).
9. Please provide the Volume and page range in ref. (Brakel and Azar, 1989)
10. Please provide the Page range in ref. (Clark, 1979).
11. Please provide the Page range in ref. (Crory, 1982).
12. Please provide the Page range in ref. (David et al., 1998).
13. Please provide the Page range in ref. (Dvorkin et al., 1991).
14. Please provide the Page range in ref. (Dvorkin et al., 1994).
15. Please provide the Volume and page range in ref. (Enen et al., 1984)
16. Please provide the Volume and page range in ref. (Eustes et al., 1994).
17. Please provide the Page range in ref. (Hartman, 1959).
18. Please provide the Page range in ref. (Hoffmann, 1912).
19. Please provide the Page range in ref. (Hustrulid and Fairhurst, 1971).
20. Please provide the Page range in ref. (Kim and Drabkin, 1995).

21. Please provide the Page range in ref. (Knight et al., 1996).
22. Please provide the Volume and page range in ref. (Long and Mitchell, 1992).
23. Please provide the Page range in ref. (Lundberg, 1973).
24. Please provide the Volume and page range in ref. (Ma and Azar, 1986).
25. Please provide the Volume and page range in ref. (McLamore, 1971).
26. Please provide the Volume and page range in ref. (Millheim, 1978a).
27. Please provide the Volume and page range in ref. (Millheim, 1978b).
28. Please provide the Volume and page range in ref. (Millheim, 1978c).
29. Please provide the Volume and page range in ref. (Millheim, 1978d).
30. Please provide the Volume and page range in ref. (Millheim, 1979a).
31. Please provide the Volume and page range in ref. (Millheim, 1979b).
32. Please provide the Volume and page range in ref. (Millheim, 1979c).
33. Please provide the Volume and page range in ref. (Millheim, 1979d).
34. Please provide the Volume and page range in ref. (Millheim and Apostal, 1981).
35. Please provide the Volume and page range in ref. (Millheim, 1978).
36. Please provide the Volume and page range in ref. (Murphey and Cheatham, 1965).
37. Please check the page range in ref. (O’Neill et al., 1990).
38. Please provide the Page range in ref. (Perry, 1992).
39. Please provide the Page range in ref. (Rémond, 2003).
40. Please provide the Page range in ref. (Rodger and Littlejohn, 1980).
41. Please provide the Page range in ref. (Salgado et al., 1997).
42. Please provide the Volume and Page range in ref. (Sifferman et al., 1974).
43. Please provide the Page range in ref. (Simon, 1964).
44. Please provide the Page range in ref. (Smith, 1960).
45. Please provide the Volume and page range in ref. (Swanson, 1994).
46. Please provide the Page range in ref. (Teale, 1965)
47. Please provide the Volume and page range in ref. (Toutain, 1981).
48. Please provide the Page range in ref. (Van den Berg et al., 1996).

49. Please provide the Page range in ref. (Vipulanandan et al., 1990)
50. Please provide the Volume and page range in ref. (Walker, 1973).
51. Please provide the Volume and page range in ref. (Walstrom, 1969).
52. Please provide the Page range in ref. (White, 1912).
53. Please provide the Volume and page range in ref. (Wolf and deWardt, 1981).
54. Please provide the Page range in ref. (Yu and Mitchell, 1998).
55. Please provide the Page range and expanded form of the journal name in ref. (Zang and Wong, 1995).